Review and prospects of magnonic crystals and devices with reprogrammable band structure

2014 J. Phys.: Condens. Matter 26 123202

(http://iopscience.iop.org/0953-8984/26/12/123202)

IOP Publishing Journal of Physics: Condensed Matter
J. Phys.: Condens. Matter **26** (2014) 123202 (32pp) doi:10.1088/0953-8984/26/12/123202

Topical Review

Review and prospects of magnonic crystals and devices with reprogrammable band structure

M Krawczyk[1] **and D Grundler**[2,3]

[1] Faculty of Physics, Adam Mickiewicz University in Poznan, Umultowska 85, Poznań, 61-614, Poland
[2] Lehrstuhl für Physik funktionaler Schichtsysteme, Physik-Department, Technische Universität München, James-Franck-Straße 1, D-85747 Garching b. München, Germany
[3] Institut des Matériaux, Faculté Sciences et Technique de l'Ingénieur, Ecole Polytechnique Fédérale de Lausanne, 1015 Lausanne, Switzerland

E-mail: grundler@ph.tum.de

Received 11 October 2013
Accepted for publication 9 December 2013
Published 6 March 2014

Abstract
Research efforts addressing spin waves (magnons) in micro- and nanostructured ferromagnetic materials have increased tremendously in recent years. Corresponding experimental and theoretical work in magnonics faces significant challenges in that spin-wave dispersion relations are highly anisotropic and different magnetic states might be realized via, for example, the magnetic field history. At the same time, these features offer novel opportunities for wave control in solids going beyond photonics and plasmonics. In this topical review we address materials with a periodic modulation of magnetic parameters that give rise to artificially tailored band structures and allow unprecedented control of spin waves. In particular, we discuss recent achievements and perspectives of reconfigurable magnonic devices for which band structures can be reprogrammed during operation. Such characteristics might be useful for multifunctional microwave and logic devices operating over a broad frequency regime on either the macro- or nanoscale.

Keywords: magnonics, magnonic crystal, reprogrammability, spin waves, reconfigurable, meta-material, nanomagnet

Contents

1. Introduction

1.1. General overview

Periodic modulation of a ferromagnetic material was considered to be a versatile concept in microwave technology almost 40 years ago [1]. For a long time, arrays of macroscopic metallic stripes or dots, etched grooves or pits, periodic variations of the internal magnetic field H_{int} and saturation magnetization M_{S} by ion implantation were among the means for creating periodic magnetic structures. Coupled to spin waves (magnons) the transmission of electromagnetic waves was thereby controlled on lateral length scales from a few hundred microns to millimeters [2, 3]. Recently, advances in nanoscience have allowed one to couple electromagnetic waves to spin-wave channels approximately 100 nm wide in individual and periodically patterned ferromagnets [4–6]. Hence, nanotechnology offers novel perspectives for microwave applications of magnons operating at the nanoscale.

From a historical point of view, spin-wave (SW) dynamics in periodically patterned ferromagnets was investigated even before the emergence of the photonic crystal in 1987 [7, 8]. After that date, research in photonics on such artificial crystals and periodically patterned dielectric materials progressed rapidly. The tailored photonic band structure with allowed minibands and forbidden frequency gaps (bandgaps) allowed the creation of integrated photonic circuits and provoked slow light in solids [9]. Thereby, unprecedented means for wave control in solids were provided, stimulating abundant new physics and many new applications [10]. A striking example is given by metamaterials exhibiting zero or negative effective refraction indices [11–13]. The concepts of artificial crystals or metamaterials developed for electromagnetic waves in the optical and microwave frequency regime were applied also to other types of waves. Periodic structures were used for molding the flow of plasmons, elastic or acoustic waves and spin waves [14]. For SWs in ferromagnets, it was realized that magnonic crystals (MCs), i.e., the magnetic analogue of the photonic crystal, form a peculiar class of artificial crystals. In their case, the band structure is not only given by the periodic patterning but depends decisively on the spatial arrangement of magnetization vectors **M** that can be changed during operation. This feature offers an additional degree of freedom for artificially tailoring wave properties in solids and has already given rise, for example, to the so-called reconfigurable artificial crystal, exhibiting a reprogrammable band structure [15]. Interestingly, research in photonics and THz wave technologies aims at reconfigurable meta-devices as well, where periodic properties of patterned materials are varied during operation. Such tunable devices are based on stretchable substrates and micromechanical platforms or incorporate microfluidic channels [16]. It is believed that reconfigurable devices offer novel perspectives for applications and multifunctional sensors.

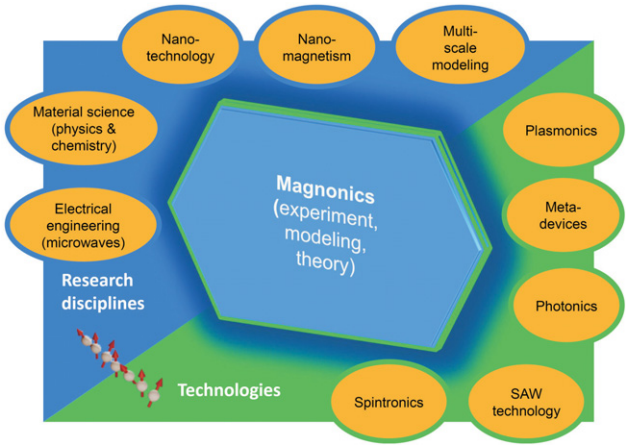

Figure 1. Magnonics embedded in a multidisciplinary research (left) and technology (right) environment. Such interconnections promise novel perspectives for fundamental research on wave properties in solids and unexplored concepts for sensing, signal transmission and data processing from the GHz to THz frequency regime.

In this topical review, we discuss the physics and recent developments in reconfigurable magnonic crystals and devices which allow unprecedented control of spin waves from macroscopic to microscopic length scales. So far, current-carrying leads and magnetic fields have mainly been used to control magnetic states and thereby the dynamic response. This power-consuming approach needs to be overcome in the future. But indeed, more advanced control mechanisms are readily available based, for example, on ferro- or piezoelectricity [17]. Reconfiguration might then be achieved at both short timescales and low power consumption. At the same time, it is predicted that precisely defined periodic lattices of nanomagnets support nonreciprocal signal transmission, being relevant for microwave isolators and circulators operating on the micro- and nanoscale [18]. Recently discovered magnetic lattices created by skyrmions and artificial spin ice are expected to fuel further research on magnonic crystals. We cover such aspects in that we discuss multidisciplinary research connecting magnonics to different disciplines and technologies (figure 1).

1.2. From periodic media concepts to magnonic crystals

Depending on the wavelength λ, metamaterials have been created in mainly two subgroups. Following [19], they form either bandgap materials which are described by Bragg reflection and other periodic media concepts (if λ is on the order of the periodicity a), or artificial materials which are described by homogenization and effective-media concepts (if λ is much longer than a). Photonic crystals that exhibit an artificially tailored band structure for electromagnetic waves with allowed minibands and forbidden frequency gaps fall into the subgroup of bandgap materials. The corresponding man-made properties have fueled photonic technologies [20]. We focus on this subgroup in the following for our review on magnonics. Reconfigurable effective-media for spin waves have not yet been largely addressed [21–23].

In periodic media (figure 2), waves in general undergo two opposing microscopic mechanisms for band formation.

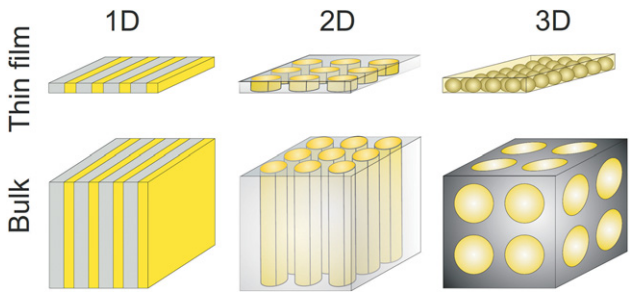

Figure 2. Classification of magnonic crystals as used in this review. Depending on the dimensionality of the system, i.e. the number of dimensions at which parameters vary, MCs can be one- (1D), two- (2D) or three-dimensional (3D) (first, second and third column, respectively). Thin-film MCs (top row) exhibit confined modes in the vertical direction and extend in the horizontal plane. Bulk MCs (bottom row) are assumed to fill the whole space, such that conceptually the external shape does not play a role in demagnetization effects.

On one hand, starting from confined or standing modes in individual resonators, coherent coupling between them allows the creation of dispersive bands. The discrete eigenfrequencies f transform into dispersion relations $f(k)$ that support propagating waves from resonator to resonator if arranged on an appropriate lattice ($k = 2\pi/\lambda$ is the wavevector). On the other hand, waves can undergo coherent scattering and Bragg reflection in a periodically modulated material, giving rise to a modified band structure with partial or complete band gaps. The eigensolutions of the wave equation fulfil Bloch's theorem in either case and, regardless of the type of excitation, form the band structure in reciprocal space. The artificially tailored minibands and bandgaps then allow one to tailor the phases and velocities of propagating waves via geometrical parameters. The detailed shape of the band structure and its sensitivity to the structure and material parameters depend on the wave type.

Spin waves exhibit very interesting dispersion relations $f(k)$ already in plain films even if the films are magnetically isotropic. In a complex form, they depend on (i) the wavevector **k**, (ii) the strength and (iii) orientation of the external magnetic field **H** with respect to **k**. (iv) The shape of the magnet and (v) magnetocrystalline anisotropy add further important parameters for $f(k)$ [24–28]. Consequently, the band structure of magnonic crystals created from ferromagnets is influenced by many additional factors apart from those that MCs have in common with other types of artificial crystals, i.e., the lattice symmetries and geometrical parameters given by the periodic patterning. In this paper we concentrate on magnonic crystals as they promise the most comprehensive control over relevant properties such as frequency, phase, velocity, amplitude and nonreciprocity [18] in magnonics. In this relatively young research field one aims at using SWs for carrying and processing information [29–33].

Magnonic crystals are magnetic materials with a periodic distribution of different materials or specific material parameters (e.g. saturation magnetization M_S or magnetocrystalline anisotropy), or other modulated parameters (such as external magnetic field or stress) modifying the propagation of SWs. Regardless of the nature of the periodic distribution, MCs can be divided into two main classes, finite-thickness and bulk MCs (figure 2). For both classes, MCs can be specified with one- (1D), two- (2D) or three-dimensional (3D) properties. The classification given here does not exhaust the possible forms of MCs, but provides a scheme for systematic studies of the dynamic properties of spin waves in MCs.

When combined with nanoscience and nanotechnology, magnonics allows one to create, for example, microwave devices operating at the nanoscale—that is, devices on length scales about four to five orders smaller than the wavelength λ of GHz electromagnetic waves in free space. The advantages of magnonics over photonics and electronics include scalability impossible with electromagnetic waves, and low energy consumption and fast operation rates compared with electronic devices, respectively [31, 34]. Besides, spin waves allow easy tunability by an external magnetic field and, as will be stressed here, reprogrammability. This makes magnonics interesting for a number of other fields of nanoscience and nanotechnology, because of the potential integration, for example, with semiconductor technology and spintronics (figure 1).

Parameters (ii)–(v), being of relevance for the magnonic band structure, might be varied for a given magnonic device in a quasi-continuous manner by external means. They allow one to shift eigenfrequencies f up or down and change the group velocity $v_g = 2\pi\partial f/\partial k$. This large tunability by itself goes beyond the possibilities, for example, in photonics and plasmonics. In section 3 we will argue that different magnetic states add a peculiar degree of freedom in that they allow one to reconfigure the dynamic response. Even more strikingly, for a given magnonic crystal the magnetic periodicity in real space, and thereby the Brillouin zone (BZ) boundary in reciprocal space, can be reprogrammed on purpose. We will review the state of the art, and summarize the advantages and drawbacks.

We will not describe the methods used for calculating magnonic band structures, fabricating samples or measuring the dynamic properties of magnonic crystals, for example, by Brillouin light scattering (BLS), ferromagnetic resonance (FMR) or all-electrical broadband spin-wave spectroscopy using coplanar waveguides (CPWs). Materials that have been exploited so far the most for magnonics are yttrium iron garnet (YIG) in macroscopic devices [30] and metallic ferromagnets such as $Ni_{80}Fe_{20}$ (Permalloy), Co and CoFeB in micro- and nanostructured devices. Among these materials YIG, as an insulating ferrimagnet, is known to exhibit the smallest SW damping, corresponding to decay lengths of several 100 μm and beyond [30]. Metallic ferromagnets such as, for example, Permalloy and CoFeB provide much shorter decay lengths but are often used for magnonic prototype devices due to compatibility with nanotechnology. Further details can be found in the literature [29–33]. The paper is organized as follows. First we review the literature from the point of view of each class of magnonic crystals (figure 2). Sections 2–4 provide an overview of research on thin-film (figure 3) and bulk MCs. Prospective directions of research, in particular regarding reprogrammable MCs and interconnected research disciplines (figure 1), are discussed in sections 3 and 5. Section 6 provides a brief summary of the paper.

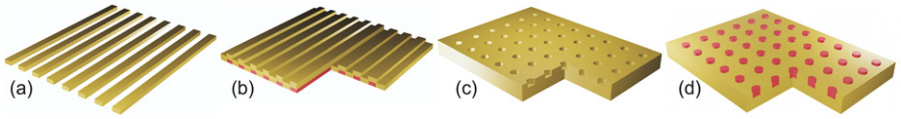

Figure 3. Sketches of thin-film magnonic crystals. (a) Array of ferromagnetic stripes to be coupled dipolarly via air gaps and (b) a continuous film with one or two corrugated surfaces (red stripes represent either the same material or a different magnetic or nonmagnetic template). (c) Arrays of empty holes forming a magnetic antidot lattice and (d) holes refilled by a different ferromagnet forming a bi-component MC. Here we depict square lattices, but other Bravais lattices have already been addressed as well.

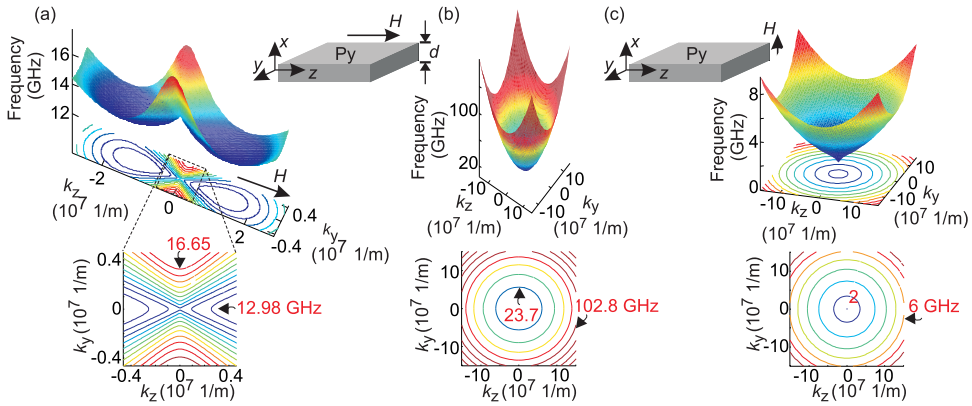

Figure 4. Dispersion relations of spin waves as a function of in-plane wavevectors (k_y and k_z) in a thin film of Py of thickness (a) 50 and (b) 1 nm. The in-plane magnetic field $\mu_0 H$ is 0.2 T in (a) and 0.02 T in (b). (c) Dispersion relation of a 50 nm thick Py film in an out-of-plane magnetic field of 1.5 T. The insets in the bottom row show contours of constant frequency in k-space (isofrequency plots). In (a) a strongly anisotropic dispersion of SW is characteristic for the magnetostatic part of the dispersion relation. The circular contours in (b) are characteristic for the exchange-dominated spin waves at high frequencies. The isotropic and linear dispersion in (c) is characteristic for magnetostatic spin waves subject to an out-of-plane magnetic field. The calculations are performed with the analytical formulas for SW dispersion relations taken from [28].

2. Thin-film magnonic crystals

Magnonic crystals with thin-film geometry (figure 3) are particularly interesting for discussing band formation mechanisms that go beyond photonics and plasmonics [29, 32, 33, 35–37]. For this, it is instructive to revisit the dispersion relations and contours of constant frequency (isofrequency contours) in homogeneous and saturated thin films (figure 4). They serve as a starting point for the analysis of SW propagation in thin-film MCs. Usually three geometries are distinguished, i.e., the Damon–Eshbach geometry (DE), backward volume magnetostatic wave geometry (BVMW) and forward volume magnetostatic wave geometry (FVMW). In the DE and BVMW geometries, a magnetic field **H** is in the plane of the film, and propagation of SWs is perpendicular and parallel to the direction of the magnetization **M** in figures 4(a) and (b), respectively. In FVMW geometry the magnetic field **H** is perpendicular to the film plane (figure 4(c)). The wavevector regime where exchange interaction dominates over dipolar interaction is extracted from these diagrams by considering that exchange-dominated spin waves follow a parabolic dispersion. Exchange interaction is dominant in figure 4(a) for $k_y \geq 10^7$ m^{-1}, in (b) for all considered wavevectors and in (c) for in-plane wavevectors larger than 10^7 m^{-1}.[4] At small k, linear dispersion relations are seen in figures 4(a) and (c). This wavevector regime is defined as the so-called magnetostatic regime.

For a given material and film thickness, the lattice constant a of the MC determines whether the first BZ boundary (e.g., π/a for a linear chain or square lattice of magnetic elements) is in the magnetostatic or exchange-dominated regime. For relatively large (small) lattice constants a, back-folding happens in the anisotropic magnetostatic (isotropic parabolic) regime of $f(k)$.

For MCs, the most involved and anisotropic band structures are known for in-plane magnetization and magnetostatic SWs. This is highlighted in figure 5, where broken lines indicate the dispersion relations $f(k)$ for two orthogonal directions of a 20 nm thick Py thin film subject to an in-plane field of 0.02 T. Note that, depending on the direction of **k**, the group velocity v_g near the Γ point ($k = 0$) is either negative (BVMW geometry) or positive (DE geometry) (figure 5(a)). In the presence of a 2D periodic lattice (figures 5(b) and (c)) back-folding of the anisotropic branches $f(\mathbf{k})$ occurs such that complex band structures are formed (figure 5(d)). Numerous modes (figure 5(e)) are thereby formed in the center of the first Brillouin zone. For SWs in thin films with out-of-plane magnetization, the isofrequency contours are in contrast isotropic, mimicking the case of electromagnetic waves in an isotropic dielectric medium. In the following we discuss different thin-film MCs, addressing the different degrees of complexity in a sequential manner.

[4] Note that the lowest-energy SW confined as a standing wave in the x direction is at high frequency outside figures 4(a) and (b).

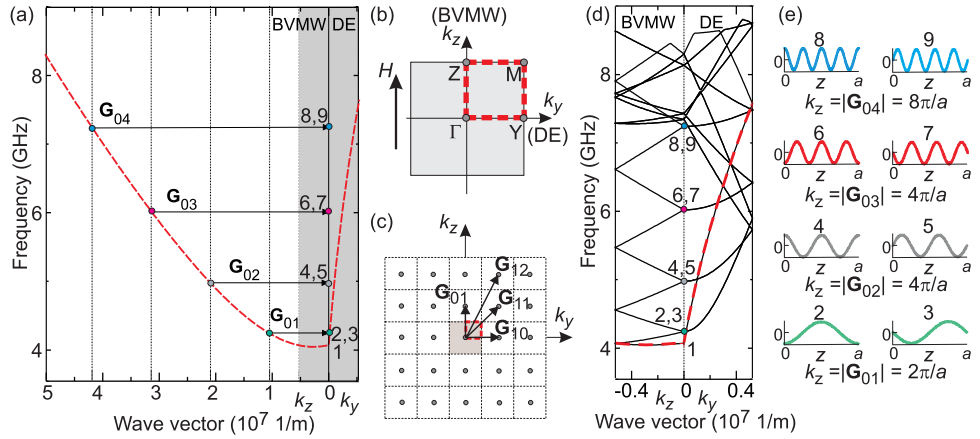

Figure 5. (a) Dispersion relations (dashed lines) of SWs in a homogeneous ferromagnetic thin film with in-plane magnetization ($\mu_0 H = 0.02$ T). Branches are shown along the k_z and k_y directions described in (b), i.e., in the BVMW and DE geometry, respectively. Vertical dotted lines in (a) show positions of the reciprocal lattice vectors **G** along the z axis as introduced by a 2D periodic lattice in (b) and (c). The gray-shaded area marks the first Brillouin zone (BZ) that would follow from a periodicity of 600 nm. (b) First BZ of a square lattice 2D MC with indicated high-symmetry points Γ, Y, M and Z in the center and at the boundary of the first BZ. We distinguish the two directions of the wavevector **k** along the bias magnetic field and perpendicular to it, i.e., the BVMW and DE geometry, respectively. (c) Periodic representation of the reciprocal space with a few reciprocal lattice vectors ($\mathbf{G}_{10}$, $\mathbf{G}_{11}$, $\mathbf{G}_{12}$ and $\mathbf{G}_{01}$) for the 2D MC with a square lattice. The gray-shaded area marks the first BZ shown in (a). (d) Magnonic band structure in the first BZ for the homogeneous film with the artificial periodicity introduced (the lattice constant is $a = 600$ nm), i.e., the empty lattice model (ELM). The part of the dispersion from (a) in the first BZ is marked by a bold dashed line (red online). The low-frequency branches along k_z are formed directly by shifts (back-folding) of the SW dispersion relation from higher-order BZs. The frequencies in the BZ center ($k = 0$) are obtained by shifts according to the arrows shown in (a). (e) The spin-precessional amplitudes of SWs at the center of the BZ as derived from the ELM (modes 2–9). The amplitude is plotted in the unit cell (side length a) along the direction of the static magnetic field, i.e. along the z-axis. The respective value of the wavevector is written below each mode. Data taken from [38].

2.1. 1D thin-film magnonic crystals

1D thin-film MCs (thin films periodically patterned in one lateral dimension) and waveguide structures fall into the definition of figure 2 (top left). Planar 1D magnonic crystal were studied in the form of arrays of alternate stripes of ferromagnetic and nonmagnetic materials (figure 3(a)) [39–45], stripes of two different ferromagnetic materials (bi-component MCs) [45–47] and structures with more complex unit cells including more than one material [48, 49]. A 1D MC consisted also of a continuous film with periodically modulated magnetic properties, such as the magnetic anisotropy or saturation magnetization [50, 51]. One-dimensional periodicity was introduced externally in a homogeneous film, for example, by current-carrying metal stripes on top of a ferromagnetic film provoking a periodic magnetic field of spatially varying strength or orientation [52–55]. Waveguide structures included chains of dots [56, 57] and single stripes with a periodically modulated width and SW propagation along the stripe axis [58, 59]. Such subgroups of MCs are described below in sections 2.1.5 and 2.1.6, respectively. Magnonic crystals with corrugated surface (figure 3(b)) are classified under 3D thin-film MCs.

2.1.1. Array of stripes. Artificially tailored SW dispersion relations (magnonic bands) in 1D arrays of long stripes were confirmed using wavevector-resolved BLS [39]. The experimentally studied thin-film 1D MCs consisted mostly of stripes with a width of a few hundred nm and edge-to-edge separations of 100 nm and below. In the initial studies the stripes were magnetized along the long axis. Propagating spin waves were observed for a wide range of angles between the propagation direction given by **k** and the long axis of the stripes [42]. In particular, partial magnonic bandgaps were observed [42, 44]. The miniband width of the lowest-frequency mode was found to be largest and so was the group velocity v_g. In the following we discuss band formation for 1C MCs subject to magnetic fields applied in different in-plane and out-of-plane directions.

Magnetic field along the stripes. Generally, ferromagnetic stripe arrays are a powerful concept to investigate dynamic coupling between individual SW resonators that leads to the formation of dispersive magnonic bands [40, 60]. When stripes are long and the magnetization is aligned with the long axis, static demagnetization effects do not play a significant role. The dynamic dipolar stray fields (dipolar coupling) due to precessing magnetic moments provide the relevant interaction being responsible for collective SW excitations across the array. In nanostripes, magnetic shape anisotropy often leads to bistable magnetic states and stabilizes the magnetization vector **M** in one of the two opposing directions along the long axis in zero magnetic field. In many investigations, SWs with wavevectors **k** transverse to the stripes have been considered, i.e., in a DE geometry, in a remanent magnetic state or in magnetic fields applied along the long axis.

Such arrays of interacting ferromagnetic stripes have been shown to form 1D MCs [37] (figure 6). The magnonic band structure depends on both the spectrum of SWs in a single nanostripe and the strength of the coupling between

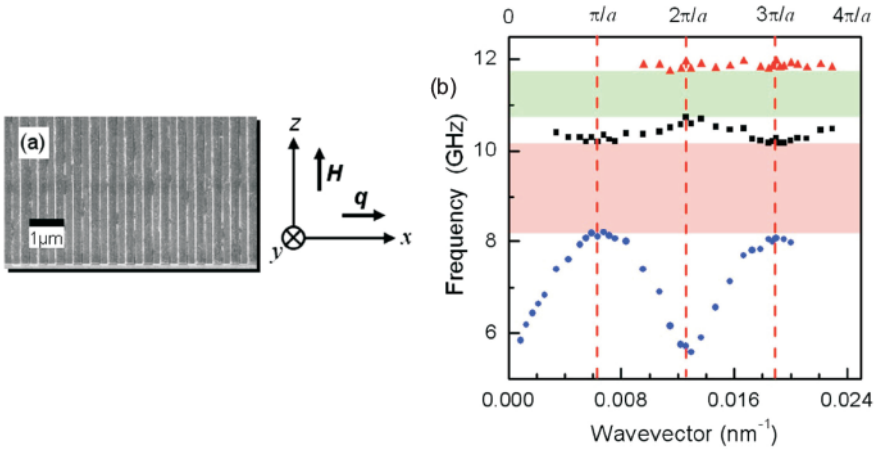

Figure 6. (a) Scanning electron image of a periodic array of 30 nm thick and 250 nm wide Py and Co stripes arranged in an alternate manner (1D bi-component MC). q denotes the wavevector. (b) Magnonic band structure measured with BLS at zero bias magnetic field after all stripes were magnetized in the same direction. The BZ boundaries are marked by vertical dashed lines and magnonic bandgaps by shaded bands. Reprinted with permission from [48]. Copyright [2009], AIP Publishing LLC.

eigenoscillations in different nanostripes. For a thin-film stripe the wavevector is decomposed into two in-plane components $k_{\parallel}$ and $k_{\perp}$, being parallel and perpendicular, respectively, to the long axis[5]. For a magnetization **M** aligned with the long axis and $k_{\parallel} = 0$, the eigenfrequencies of an individual nanostripe show a spectrum of discrete eigenfrequencies as a function of $k_{\perp}$ [61, 62]. To analyze the spin-precessional motion and band formation we subdivide **M** of a nanostripe into a static component $\mathbf{M}'$ parallel to the long axis and a dynamic component **m** precessing in the plane perpendicular to $\mathbf{M}'$ according to $\mathbf{M} = \mathbf{M}' + \mathbf{m}(t)$ ($m \ll M' \approx M_S$, t is the time). Spin precession is induced when **M** experiences a misalignment with $\mathbf{H}_{\rm int}$ following $\mathrm{d}\mathbf{M}/\mathrm{d}t \propto -\mathbf{M} \times \mathbf{H}_{\rm int}$ [28]. The misalignment might be provoked by a rf magnetic field, a field pulse, or thermal or optical excitation.

The fundamental mode is a confined mode with no nodal line and exhibits the lowest frequency (node number $n = 0$). Considering the boundary conditions, the amplitude of the dynamic component $\mathbf{m}(t)$ is in general not constant across the width of the stripe. Boundary conditions for confined modes have been introduced in [63–65]. Modes with higher frequencies have node numbers $n = 1, 2, \ldots$. Note that the boundary conditions depend on n. The eigenfrequencies are determined by many parameters, such as the shape, dimensions (thickness and width), saturation magnetization, exchange constant, magnetoelastic contributions as well as volume and surface anisotropy terms. Moreover, the spectrum and eigenmodes depend on the strength and orientation of the magnetic field **H**, as will be detailed later. When stripes are arranged closely enough the confined modes can couple via dynamic dipolar stray fields and form allowed minibands separated by forbidden frequency gaps [39].

[5] For the 1D and 2D thin-film MCs, we assume a homogeneous profile of the spin-precessional motion in the out-of-plane (oop) direction described by a wavevector $k_{\rm oop} = 0$. For 3D thin-film MCs one needs to consider $k_{\rm oop} \neq 0$.

Band widths depend again on many factors, such as the thickness and width of the stripes, the edge-to-edge separations, saturation magnetization, cross-sectional geometries, direction of **H** and the roughness. The detailed dependence of the magnonic band structure on each of the factors and combinations thereof has not been fully investigated yet. A decisive parameter is however given by the number of nodes n on which the amplitude of the dynamic stray field depends crucially. The stray field is largest for $n = 0$, and decreases non-monotonically with increasing n. This argument explains why miniband widths decrease from bottom to top in figure 6(b).

In recent years, stripes with a width w much larger than the thickness t were investigated in most of the papers. For $t \ll w$, the dynamic demagnetizing field generated by precessing spins strongly suppresses the oscillation amplitude of **m** in the out-of-plane direction, and thus renders the spin-precessional motion strongly elliptical. Since in a first approximation stray fields from precessing spins are proportional to the dynamic components **m**, the strongest coupling is expected to occur via the in-plane component [41]. While the in-plane stray field forces in-phase oscillations in the array, the small out-of-plane component of the magnetization works against such oscillations. Its effect is however much weaker. In this framework, if solely induced by the in-plane stray fields, the dipolar coupling might be relevant at short range only, especially for metallic stripes. This consideration agrees conceptually with the coherence length introduced in [15, 66] to model SW eigenfrequencies measured in 1D MCs quantitatively[6].

Qualitatively, a dispersion relation can be derived on the basis of the following arguments: in the center of the Brillouin zone (i.e. for a wavevector $k = 0$) the modes oscillate in-phase in each unit cell (the oscillations are in accordance with the in-plane dynamic stray field). At the boundary of the BZ

[6] In [15, 66] the justification for the coherence length was provided by the modification of the magnetic properties at rough edges of real stripes.

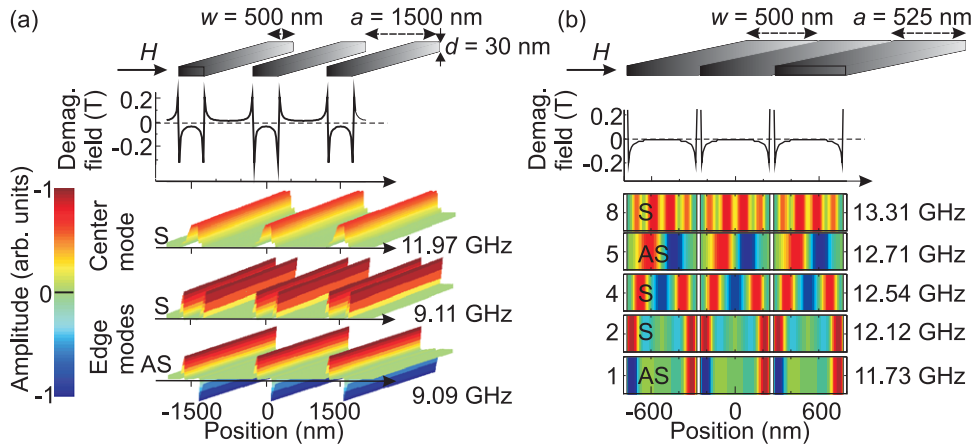

Figure 7. Amplitudes of the spin-precessional motion in a periodic array of infinitely long Py stripes calculated with the plane-wave method in the center of the BZ. The color code of the amplitudes is defined on the left. A field $\mu_0 H$ of 0.2 T is assumed in a direction transverse to the stripes. The Py stripes have thickness and width of 30 and 500 nm, respectively. We consider three unit cells of two different arrays with a period of (a) 1500 nm and (b) 525 nm. In (a), edge modes with antisymmetric (AS) and symmetric (S) edge excitations are shown. At higher frequency, the center mode is excited. In (b), the modes form more complex profiles due to dipolar coupling between the closely spaced stripes. The excitation at the highest frequency (values are given on the right) originates from the center mode without a phase change in the unit cell. Spatial profiles of the static demagnetizing fields are depicted below the stripe arrays (gray) in (a) and (b).

($k = \pi/a$) the in-plane components of **m** of neighboring stripes are in anti-phase, provoking large energy due to repulsive forces. As a consequence the SW frequency of the fundamental mode increases with k in the first BZ. At small k the slope in $f(k)$ should be linear and qualitatively similar to that of a DE mode in a homogeneous thin film. The SW group velocity v_g is nonzero in the long-wavelength limit (small k). This is in contrast to plasmons in chains of near-field coupled metallic resonators [67, 68].

The band width depends on the edge-to-edge separation. The interaction between stripes obviously increases with decreasing spacing between the nanostripes. The strength of the coupling should increase also with increasing stripe width; however, it should be remembered that changes in the width or thickness of the nanostripe affect the eigenmodes of the single nanostripe, especially the ellipticity of the spin-precessional motion[7]. Increased thickness reduces the ellipticity of precession; for $t = w$ the precession is circular; for $t > w$ a stray field of larger amplitude is created by the out-of-plane component of **m**. At a certain value of t the dynamic coupling via the out-of-plane stray field will start to prevail over the coupling via the in-plane stray field. Then, the frequency at the boundary of the BZ, where **m** in neighboring stripes oscillates out of phase, should be lower than at the center. As a consequence, a negative group velocity v_g is expected. This is an interesting effect, as a negative group velocity would be obtained in the DE geometry. Although this has not been verified experimentally yet, such behavior of the SW dispersion was observed in micromagnetic simulations for a stack of rectangular magnetic elements [69]. Here, the relation between the ellipticity of precession and the sign of the group velocity was established.

[7] For the arrays, stripes of rectangular cross section were assumed. A cross-sectional shape different from rectangular or square would imply a structural inhomogeneity along the out-of-plane direction, which by our definition is characteristic of a 3D thin-film MC.

These arguments apply to the coupling of the fundamental mode of the stripe. The mode with $n = 0$ is expected to provide the largest miniband width due to the most prominent coupling. Besides this, we point out that the dynamic dipolar coupling itself modifies the spin-precessional amplitudes and profiles, resulting in a decreased pinning of the spin waves at the edges of the stripes [41, 70]. Interestingly, the SW excitations in stripes can be also approximated by the solutions of a thin film with static effective demagnetization factors [71], yielding reasonably good results with respect to the BLS experimental data obtained on Py stripes. An opposite model was considered as well, to determine the role of the dipolar interaction in microwave-assisted switching of stripe arrays [72]. Note that unintentional edge roughness reduces the demagnetization effect and thereby the dipolar pinning at nanostripe edges as well. As a consequence, the fundamental mode is less confined and dipolar interaction between neighboring stripes is expected to increase compared to nanostripes with ideal edges.

Magnetic field in a direction transverse to the stripes. A so far less explored configuration of **M** and **k** corresponds to the BVMW geometry [44]. Here, the dynamic coupling and formation of the magnonic band structures evolve differently. The magnetization vector **M** points against the edges of a stripe and is parallel to the direction of propagation. The static demagnetizing field is inhomogeneous across the width of a stripe (figure 7(a)). This results in the occurrence of minima in H_{int} in which low-frequency SWs can localize, becoming so-called edge modes in spin-wave wells [73–75]. Edge modes of an individual stripe form pairs of excitations, being either symmetric (S) or antisymmetric (AS) with respect to the center of the stripe, as shown in figure 7(a). The frequencies of S and AS modes depend on the coupling between the spin-precessional motion localized at opposite edges. The coupling inside the stripe is promoted via dipolar and exchange interactions. The exchange interaction favors S

oscillations, and the dipolar coupling AS ones. In figure 7 the AS mode has a lower frequency than the S mode due to the dipolar interactions. In the case of compensating interactions or uncoupled edge oscillations, the frequencies of the S and AS modes would be degenerate. In the center of a stripe, the demagnetization effect (internal field) is small (large). Here, modes with an antinode, i.e., the so-called center modes, exist at high frequency (figure 7(a)).

The magnonic band structure resulting from center modes in the BVMW geometry can be elucidated qualitatively by a discussion similar to that presented above for the DE geometry. The dynamic magnetization $\mathbf{m}(t)$ lies in the plane perpendicular to the bias magnetic field. The spin-precessional motion has components along both the long axis and the out-of-plane direction. The first component does not contribute to the dynamic coupling, which means that solely the component normal to the plane is involved in the coupling of modes. This applies to any value of t unless domains are formed. Kuanr *et al* investigated arrays of 100 nm thick and 300 nm wide Py stripes with edge-to-edge separations ranging from 100 to 1000 nm [76]. Using FMR measurements, the authors substantiated the coupling in that an increased eigenfrequency of the center mode was found with decreasing edge-to-edge separation in the BVMW geometry. This trend is in contrast to stripe arrays being magnetized along the long axis in the DE geometry. Here, the eigenfrequency decreases with decreasing edge-to-edge separation.

The collective center mode in the BVMW geometry is expected to exhibit a negative group velocity since out-of-phase oscillations in neighboring stripes are favored by the dipolar coupling. For edge modes, positive or negative dispersion can be expected for AS and S oscillations, respectively; the determination of their relative positions on the frequency scale requires detailed calculations though (figure 7(b)). The large (weak) sensitivity of the edge (volume) modes to the dipolar coupling was demonstrated in FMR measurements performed on Fe stripes in [77].

Magnetic field in the out-of-plane direction. In the FVMW geometry the magnetization vector **M** is along the out-of-plane direction. The dynamic coupling between stripes occurs by the component of the dynamic magnetization **m** parallel to the lattice vector. In the limit $t \ll w$ the SW dispersion should be similar to that of the DE geometry, but with eigenfrequencies reduced by the strong demagnetizing field. In nanostripes of large thickness t (or small width w) the inhomogeneous static demagnetizing field modifies the SW oscillations within a nanostripe, and edge modes form at the top and bottom of the nanostripe at some value of t (or w). Still, the coupling between nanostripes is due to the stray field from **m** components along the lattice vector.

Note that a full magnonic bandgap is unlikely to occur in a lattice of stripes, since the allowed bands for SWs propagating along the stripes overlap with bandgaps for SWs propagating perpendicular to the stripe edges [42].

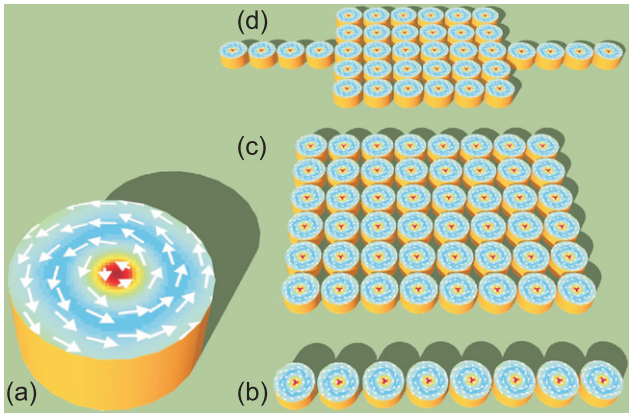

Figure 8. (a) Illustration of the simulated vortex state in a 187 nm diameter Py nanodisc (thickness of 100 nm) subject to an out-of-plane field of 0.33 T. Arrows (colors) indicate in-plane (out-of-plane) orientations of microscopic magnetic moments. In the center a vortex core is formed on a length scale given by the microscopic exchange length. In the core, moments point perpendicular to the plane. The core is surrounded by a circular flux-closure configuration. (b) 1D and ((c), (d)) 2D periodic lattices of interacting nanodiscs as discussed in [79].

2.1.2. Chain of discs. In a straight chain of ferromagnetic discs, periodicity occurs only in one direction; in the other dimensions the structure is finite. Usually the thickness of the dots is much smaller than the lateral size, and the requirement of homogeneity of the excitation across the thickness is fulfilled to a large extent. This type of structure is suitable for investigating the strength of coupling between localized SW excitations, i.e. the formation of the band structure of magnetostatic waves in dependence on the shape of the dots or their relative orientation [43, 78]. We distinguish between monodomain discs with **M** being in the plane and discs within a magnetic vortex state (figure 8(a)). Qualitative interpretation can be provided on the basis of the previous discussion of the dynamic stray fields generated by **m**. However, an applied in-plane magnetic field has components perpendicular to opposing edges of the discs. Edge modes can form near these edges and couple with similar excitations in the neighboring discs. When discs are in the vortex state (figure 8(b)) coupled gyroscopic vortex core motion can occur and provoke allowed minibands along a linear chain [79]. The relevant frequencies are typically much smaller compared to the stripe arrays. Magnonic waveguides consisting of discs were explored both experimentally by time-resolved scanning transmission x-ray microscopy and theoretically by micromagnetic simulations in [80]. Addressing 2 μm wide Py discs separated by 250 nm the relevant frequencies of coupled excitations were found to be in the 0.25 GHz regime. For the arrays, elements of rectangular cross section were assumed.

2.1.3. Bi-component 1D magnonic crystals. Bi-component magnonic crystals (BMCs) have been realized as arrays of stripes alternately prepared from two different ferromagnetic materials [48, 49]. The discussion provided in the previous sections concerning dipolar coupling applies to this scenario as well, but with an additional aspect to be taken into

consideration. If the stripes are in direct contact, the interlayer exchange interaction (i.e. the interaction between the two ferromagnetic materials) can influence the collective SW spectrum. The exchange interaction in ferromagnetic materials favors in-phase oscillations; so does the interlayer exchange interaction unless the coupling constants have opposite signs. In this case the antiferromagnetic state has a lower energy, and out-of-phase oscillations between neighboring stripes in the BMC would be favored. On the basis of this picture, the contribution of the ferromagnetic interlayer exchange interaction to the SW dynamics can be expected to have the same sign as the in-plane stray field in the DE or FVMW geometry. In the BVMW geometry the ferromagnetic interlayer exchange interaction has an effect opposite to that of the dipolar coupling provided by the out-of-plane dynamic stray field.

There is a significant difference between the dipolar and exchange interactions. The exchange interaction is strong, but has a short range. It is of importance for large values of the wavevector. Thus, the contribution of the exchange interaction is modified by changing the lattice constant. For a large lattice constant, direct exchange coupling between the ferromagnetic materials influences the magnonic band structure only slightly. It modifies the interface conditions for the SW dynamics, providing effective pinning or freely precessing spins of the magnetization at the interfaces. In MCs with a small lattice constant the exchange interaction influences the dynamics of collective SWs by defining the conditions for the formation of standing waves in a single nanostripe and thus contributing to the formation of magnonic bands. On this scale also the magnetic surface anisotropy is of importance for the magnonic band structure. The above discussion applies to the qualitative description of the magnonic bands of lowest frequencies. In higher bands, where SWs change their phase inside a unit cell on the length scale of the exchange length, the SW dispersion is determined only by the exchange interaction.

Bi-component magnonic structures have been investigated experimentally by BLS and broadband ferromagnetic resonance techniques in a lattice constant range in which the dipolar interaction predominated over the exchange interaction. The occurrence of a magnonic bandgap in bi-component magnonic crystals was first reported in [48]. The BMCs were composed of Co and Py stripes, 30 nm thick and with a lattice constant of 500 nm (figure 6(a)). The formation of the magnonic band structure (figure 6(b)) in such MCs has been shown to be of magnetostatic nature [81]. Similar characteristics were observed for SW dynamics in a Fe/Py BMC in [82]. The dependence of the band structure and bandgap widths on the lattice constant and filling fraction was studied systematically in [49]. The Co/Py stripes presented in [48] were later used for studying many different aspects related to the dynamics of SWs in BMCs [46, 81, 83, 84]. These include the influence of the boundary conditions at the interfaces between Co and Py [83], the use of these structures as reprogrammable devices [84] discussed in detail in section 3, and the effect of surface metallization on the magnonic band structure [85].

A decreased lattice constant results in an increased wavevector k_{BZ} at the boundary of the first Brillouin zone, possibly reaching the regime of exchange-coupled spin waves. In this regime, structures consisting of alternating Co and Ni stripes were considered theoretically in the DE and BVMW geometry in [47, 86]. In the DE geometry broad magnonic bandgaps with a width of tens of gigahertz were found to occur. For a lattice constant of the order of 20 nm the gap width proved independent of the magnitude of the magnetic field. For small lattice constants, SWs at the boundary of the BZ exhibit spin-precessional amplitudes that are out-of-phase in neighboring stripes. They are at high frequency due to an increased exchange energy, as the exchange interaction favors the parallel alignment of spins. The exchange energy is smaller when the unit cell is larger, in which case both the bands and the bandgaps are narrower. At a certain unit-cell size the effects of the exchange and dipolar interactions are of comparable strength. Overall, the width and center frequency of the magnonic bandgap were found to decrease significantly with increasing lattice constant in [47, 86].

2.1.4. SW waveguides based on MCs. In this section we address SW waveguides and thin-film structures in which the width modulation perpendicular to the direction of propagation plays an important role. Compared to homogeneous and straight waveguides, magnonic-crystal-based waveguides have a number of advantages related to their filtering properties [58, 87–89], i.e. their ability to act as band-pass or band-stop filters, the possibility of creating monomode waveguides which can increase the transmission efficiency, or bending waveguides with suppressed energy leakage, similarly to what has been obtained in photonic waveguides. The considered structures have different periodicities and include homogeneous stripes incorporating comb-like structures [89], a regular array of curved segments [90], stripes with periodic corrugation along the width or thickness, a line array of holes (antidots) [91] and structures with periodically modulated magnetization [51] or H_{int} [55].

Analytical models have been developed and used for the investigation of the basic properties of SW waveguides of various kinds. The models are valid under specific assumptions; typically, SW excitations are assumed to be uniform across the thickness of the waveguide and to occur in the exchange regime [92]. A curvature introduced in a narrow waveguide made of a homogeneous ferromagnetic material has been shown to provide different conditions for exchange modes than the straight parts of the waveguide. Periodic repetition of curved parts allowed the formation of a tailored magnonic band structure with bandgaps [90]. Comb-like structures and networks of magnetic nanoclusters were proposed as model systems of magnonic circuits, and their possible application as filters, interferometers and multiplexers for SWs was considered theoretically [89, 93, 94].

Other types of MC-based waveguides were investigated by numerical calculations. Periodic modulation of the stripe width has been demonstrated to open magnonic bandgaps in the transmission spectrum [95, 96]. Gaps originate either from Bragg scattering or interactions between different families of width-quantized standing waves. A combination of waveguides with different periodicity was proposed for creating

narrow band-pass filters [87]. These simulations were performed with both the dipolar and exchange interactions taken into account; however, the bandgaps were mainly determined by the exchange interaction.

In the DE configuration, with the magnetic field normal to the waveguide axis, two kinds of modes—the center and edge modes—can undergo band formation. Corrugation provided by width modulation can introduce back-folding effects to both kinds of modes [58]. The band structure depends on the size of the waveguide, the periodicity and the modulation depth. The bandgap formation was studied experimentally in waveguides of micrometer size (lattice constant of 1 μm and width modulation of 1 μm [97]). Step-like and sinusoidal modulation of the width were modeled and the theoretical results compared with experimental data [59]. Step-like modulation proved more efficient for the generation of multiple bandgaps in the DE geometry. Direct guiding of SWs with an MC-based waveguide was investigated in [98]. However, research is still at the infancy stage because of difficulties in the miniaturization and injection of SWs into such waveguides [98].

Periodic sequences of holes along a ferromagnetic stripe have been shown to offer a wide range of tunability for SW guiding [99, 100]. Arranged in one or two rows, the antidots provoke single-mode transmission bands, allowing the suppression of energy leakage. Calculations have been performed for small lattice constants (up to tens of nanometers), implying the predominance of the exchange interaction. The boundary conditions were demonstrated to significantly influence the magnonic band structure. Surface pinning of spins was shown to facilitate the opening of the magnonic bandgap.

Another interesting class of 1D magnonic crystals includes those based on a homogeneous ferromagnetic thin film with externally introduced periodic properties. Two approaches will be considered in the following, a periodic magnetic field and a metal grating deposited on a ferromagnetic film. In the former case the periodic field penetrates the film completely, whereas in the latter case only the surface and the space above the ferromagnetic film is modified.

2.1.5. Tunable periodic modulation of the internal magnetic field. A periodic bias magnetic field has been applied to a homogeneous thin film by different research groups in recent years. A current-biased meander-type wire on top of a thin ferromagnetic stripe modulated H_{int} [55] and resulted in the occurrence of magnonic bandgaps. Intriguing physics is offered by creating dynamic magnonic crystals even after a given SW has already been injected into the ferromagnet. The dynamic MC allows frequency shifts, pulse compression and beam extension. To study such effects a microwave current has been applied to a meander-type wire [52–54].

2.1.6. Metal grating on top of a thin film. Already in the 1970s, a metallic grating placed on top of a μm thick YIG film was found to generate bandgaps in the spectrum of magnetostatic waves [101–103]. The metal lines modify the electromagnetic boundary conditions relevant for the dynamical stray field generated by the magnetostatic wave propagating in the ferromagnet. This modification is sufficient for coherent scattering and the opening of band gaps. Additionally, the evanescent part of the magnetic field outside the film penetrates the grating with a finite conductivity, which increases the losses of the magnetostatic waves. The possibility of creating a band-pass filter tunable via a magnetic field was considered as early as 1977 [101]. It was also then that, probably for the first time, oblique incidence of magnetostatic waves on periodic gratings was considered. A similar configuration was developed later and is still timely research in magnonics with regard to the developed theoretical methods [104], experimental setups and potential applications. Magnonic crystals created by metallic gratings were proposed as very sensitive magnetic field sensors [105, 106]. They were also used in the studies of nonlinear effects in magnonic crystals, summarized in section 5.1. Metallic gratings which were periodic in two lateral directions were addressed theoretically and experimentally in [107]. Rejection bands were found in experiments performed on a ferromagnetic film being covered by a 2D array of metallic dots [3].

Metallic overlayers provoke nonreciprocal spin waves, especially in the DE geometry. Nonreciprocity of the spin-wave damping was predicted for ferromagnetic films with a metal grid of finite conductivity in [108]. The influence of nonreciprocity on the SW Bragg resonances in YIG films with a lattice of etched grooves was studied experimentally in [109–111]. It was shown that for a structure with a dielectric spacer between metal and corrugated YIG film, the Bragg resonances appear for large wavevectors, i.e. when the SW dispersion is already reciprocal. Recently, the nonreciprocal property in MCs was predicted to result in indirect magnonic gap openings inside the BZ [112].

2.2. 2D thin-film MCs

Two-dimensional thin-film MCs are divided into three main classes, discussed in the following sections: interacting arrays of ferromagnetic discs [29, 57, 113, 114][8], antidot lattices [115, 116] and bi-component MCs [117–119].

2.2.1. 2D arrays of ferromagnetic discs. The discussion of arrays of ferromagnetic discs follows similar arguments to those for arrays of stripes. One needs to consider however that, for 2D structures in the saturated state, static demagnetizing fields are to be taken into account. The main properties of the SW spectrum can be qualitatively explained by analyzing the dynamic stray field generated by the precession of the magnetization vectors [120]. The formation of the magnonic band structure is provoked by dynamic dipolar interactions between standing waves in the nanodiscs (often considered with M saturated in an in-plane direction) [121–123] or between gyroscopic modes of the vortex core motion, if the discs are in the vortex state [124–128]. The bands generated from standing SWs of the individual Py element and gyroscopic modes reported so far lie in different frequency regimes, typically above (figure 9) and below roughly 1 GHz, respectively. In both cases the magnonic band width is a direct measure of the

[8] In the following we use the term disc when addressing thin-film magnetic elements since circular thin-film elements have been considered in most of the works. However, the footprint might even be an oval or a square in some works. In such a case, configurational anisotropy might be considered. Similar aspects are relevant for the shape of holes in antidot lattices.

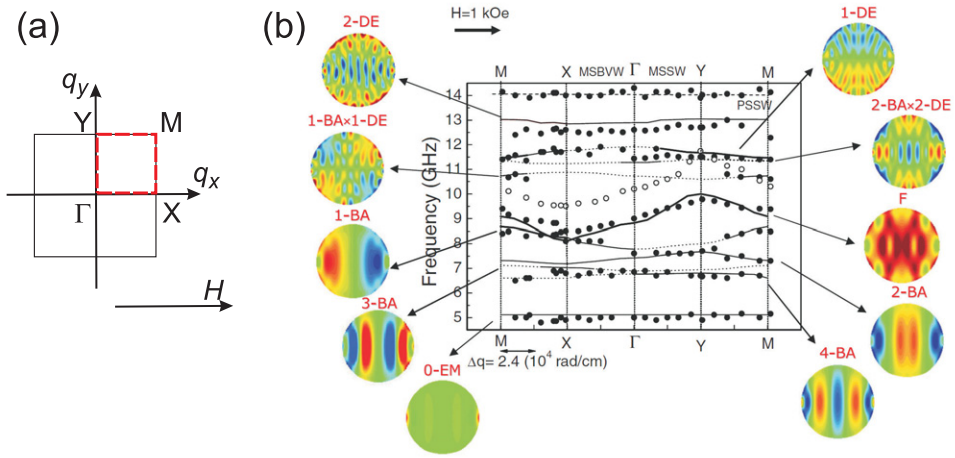

Figure 9. (a) First Brillouin zone of a 2D square lattice with the irreducible paths along which the magnonic band structure is studied in (b). (b) Magnonic band structure of a square lattice of Py discs: BLS data (filled symbols) and calculated results of the dynamical matrix method (solid lines). Open symbols show the anisotropic dispersion relation measured on the unpatterned film. Here the spin-wave wavevector is denoted by q. The discs are arranged in the x, y plane. Magnetostatic backward volume wave (MSBVW) and magnetostatic surface wave (MSSW) geometries were addressed, corresponding to BVMW and DE geometries, respectively, as defined in this review. PSSW indicates the first perpendicular standing spin wave. Bold, solid and dotted lines refer to modes whose calculated cross section is comparable, smaller and vanishing, respectively, with respect to that of the mode labeled with F. DE, backward-like (BA) and edge (EM) modes are specified in the profiles of the spin-precession motion shown as insets. The number of nodes is given in the labels. Red (blue) color stands for positive (negative) amplitude of the real part of the out-of-plane component of **m**. Reprinted figure with permission from [126]. Copyright (2004) by the American Physical Society.

strength of coupling, which depends on the shape of the discs, their size in relation to the spacing, the lattice symmetry, the roughness of the edges, the magnetic configuration and the spectrum of eigenmodes of the individual element [129–131].

The SW dynamics in an array of magnetic nanodiscs with in-plane magnetization is significantly anisotropic. The magnonic band structure of SWs in a square-lattice-based array of magnetically saturated circular discs has been determined over the whole irreducible part of the first BZ recently in BLS experiments (figure 9). Good agreement with calculated results has been reported [126]. For a given direction of the in-plane bias magnetic field, the dispersion of long-wavelength SWs originating from the fundamental eigenoscillation changes from a positive group velocity for wavevectors perpendicular to **H** to a negative one for **k** parallel to **H**. Weak and strong coupling is seen to occur in the directions parallel and perpendicular to the external magnetic field, respectively [132]. It has been pointed out that in the BVMW geometry the experimental observation of the magnonic band structure is challenged by the formation of standing spin waves [133]. The rule that coupling of SW excitations is efficient for spacing between discs being smaller than the disc diameter was established phenomenologically [134]. A significant modification of the fundamental mode in the DE geometry is expected to occur in the square array of ferromagnetic discs with decreasing lattice constant, as predicted by the dynamical matrix calculations and confirmed by BLS measurements [135].

In hexagonal arrays of discs the dispersion is anisotropic as well [136]. In that case strongly asymmetric behavior was observed for two orthogonal directions of the magnetic field for SWs propagating in the direction perpendicular to the bias field. Collective magnonic excitations have been investigated in arrays with various lattice symmetries and elements of various shape [113, 137, 138], showing major differences between excitations of individual elements and collective excitations of the array. In these works, only selected single-element eigenmodes have been found to provoke collective SW excitations in an array. These split into multimode excitations depending on the shape and size of the element, its magnetic configuration, the edge-to-edge separation and arrangement in the array. The collective excitations can be influenced also by dephasing of the spin-precessional motion in neighboring elements of an array, leading to additional damping [137]. An in-plane rotation of the external magnetic field modifies the band structures, since different directions of the magnetic field are not equivalent in 2D arrays. Reorientation of **H** affects both the demagnetizing field inside the discs and the interaction between the elements [139]. Arrays with complex unit cells of Py nanoelements, giving rise to so-called 'non-collinear' bi-component artificial crystals[9], have been prepared recently [78]. Band structures in in-plane fields have not yet been presented, but studies addressing the out-of-plane direction of **M** suggest miniband formation [140]. Considering 30 nm thick Py, an edge-to-edge separation of 50 nm and a lattice constant on the order of two to three micrometers, the authors derived a miniband width of up to 0.14 GHz for FVMWs. This value is about an order of magnitude smaller compared to nanostructured 2D antidot lattices [116]. The small miniband width suggests a small dipolar coupling in the complex 2D lattice.

[9] Here, the term bi-component did not refer to two different materials but to two different orientations of identical stadium-like nanomagnets forming the unit cell of the periodic lattice.

Note that the magnonic band structures discussed in this section are different from the exchange-dominated SW spectra [47] which can be realized in antidot lattices and bi-component MCs prepared from two materials being exchange-coupled. Such devices will be discussed in the following.

2.2.2. Antidot lattices. Spin-wave dynamics in magnetic antidot lattices (ADLs) (figure 3(c)) has been investigated by similar techniques as for 1D MCs and 2D disc arrays. The experimental techniques include BLS [141, 142], broadband and cavity-based FMR [142–150]. Theoretical formalisms were based on micromagnetic simulations [151, 152], the dynamical matrix method [115, 153], as well as the plane-wave method [154].

In-plane fields. In in-plane magnetized ADLs the magnonic band structure is determined by the demagnetizing magnetic field (which is periodic in the plane of the film), the magnetostatic and dynamic dipolar interaction [115, 150, 154–156]. Magnetic anisotropies provoking easy and hard axes in the patterned film [157] depend on the lattice type. The shape of the holes plays an important role in the formation of the magnonic band structure [6, 142, 158]. The SW dynamics exhibits a significant anisotropy that has been measured and verified by calculations [159]. The anisotropy can have two origins: the nature of the spin-precessional motion or the lattice symmetry. The opening of bandgaps at the boundary of the BZ was found in BLS measurements and interpreted in terms of Bragg scattering by the dynamical matrix method [160].

In tangentially magnetized and saturated ADLs the internal field H_{int} is inhomogeneous and takes small values at the edges of the holes. Here, low-frequency spin-wave modes have been found to localize [141, 145, 147, 161–164]. In [165] more than one edge mode was observed in a Py-based lattice of relatively large square holes with a side length of 500 nm and a lattice constant of 1000 nm. When the holes were large enough compared to the lattice constant, the dynamic coupling between adjacent edge modes modified the magnonic bands [6, 154]. The frequency of the band formed by edge modes in a square-lattice ADL was lower than the uniformly precessing mode of the homogeneous film and the group velocity of the SWs exceeded the thin-film value in the DE geometry at the same H [154]. By rotating the external magnetic field, the coupling strength between edge modes was significantly varied [154]. The character was changed from propagating to localized modes not only in the square but also in a rhombic ADL [6]. Note that in weak fields H, the nonuniform magnetization can additionally provoke different kinds of confined SW modes [166, 167]. Overall, the character of the modes (propagating versus confined) as well as the magnonic band structure were found to vary decisively with the lattice type [142], lattice constant [154], size and shape of the holes, orientation of the magnetic field with respect to high-symmetry and propagation directions, and the magnitude of the bias magnetic field [148]. Also binary antidot lattices, with two holes of different diameter in the unit cell, were investigated recently. Such a unit cell introduced additional confinement of SW modes and gave an extra degree of freedom in the design of the magnonic band structure [168, 169]. In thick ADLs, standing spin waves across the thickness were in the same frequency range as the propagating SW bands, leading to a complex dynamic response [170].

The above description of the magnonic band structure applies to the low-frequency part of the SW spectrum in which the SWs have a magnetostatic character. In the case of small lattice constants, the frequency of the first band is high at the boundary of the BZ and the exchange interaction predominates. Then the magnonic band structure is determined by scattering of spin waves on the lattice of rigid centers rather than on the inhomogeneous H_{int} [99, 100]. The magnonic bands are parabolic, and the dispersion is almost symmetric in the plane of propagation.

Out-of-plane fields. The FMVW geometry, with the bias magnetic field normal to the plane of the film, gives an opportunity for investigating a magnonic band structure in an isotropic scenario much closer to that of photonic crystals [20]. Thin-film magnonic crystals based on an antidot lattice in this geometry have already been considered by different groups [116, 171]. In [116] micromagnetic simulations showed that a permalloy ADL with a hole diameter of 120 nm possessed magnonic bandgaps for various lattice constants ranging from 180 nm up to 800 nm. The width of the gap decreased with increasing lattice constant of the square lattice of circular holes. The study was performed for wavevectors along two high-symmetry directions. In figures 10(a) and (b) we show plane-wave-method calculations of the magnonic band structure of a CoFeB-based ADL, where holes have a diameter of 200 nm arranged on a square lattice. We address the irreducible part of the first BZ fully in figure 10(b) for a lattice constant of 610 nm. Interestingly, the contours of constant frequency for the first magnonic band exhibit a circular shape in the long-wavelength limit. The contours are transformed into a square with rounded corners for increasing frequency. Just above 12 GHz the curvature of the contours changes in sign. A complete bandgap is not found. To create a complete band gap it is decisive to increase the hole diameter beyond some threshold value. This is highlighted in figure 10(d) for antidots with a diameter of 240 nm sustaining a forbidden frequency gap across the whole BZ. This prediction has not been verified experimentally yet.

Recently, SW guiding in the FMWM geometry was identified within a defect line created by a row of holes that was missing in a square ADL prepared from CoFeB. Such magnonic-crystal-based SW wave guides had an advantage over a single-stripe-based SW waveguide with a nominally identical width, in that the SW velocity was relatively large. The increased velocity was attributed to the weak lateral confinement and a SW amplitude decaying into the surrounding MC [172].

2.2.3. Bi-component 2D magnonic crystals. Composed of two different and periodically arranged ferromagnetic materials, nanoscale bi-component magnonic crystals (BMCs) have been realized in 1D and 2D configurations [49, 118, 119, 173, 174]. The BMCs consisted of periodically alternating stripes of Co and $Ni_{80}Fe_{20}$ and a lattice of Co or Fe nanodiscs of diameter $2R$ embedded in Py, respectively (figure 3(d)). The band structures of BMCs exhibit properties similar to those of 2D disc

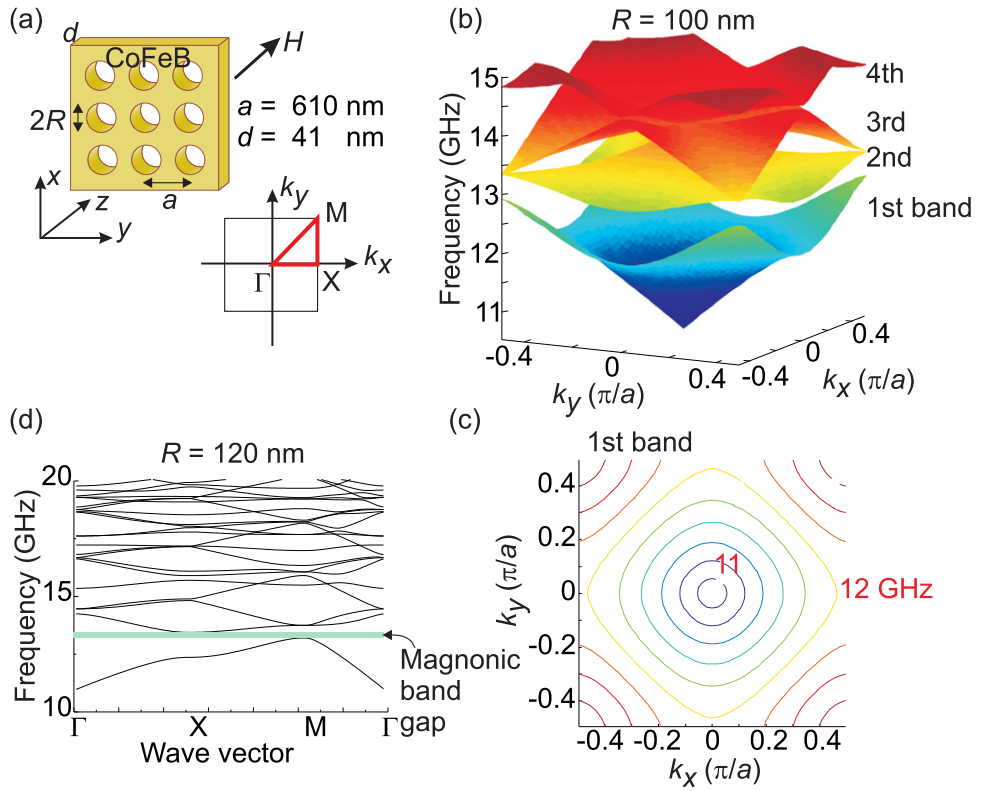

Figure 10. (a) Antidot lattice with a square array of holes and the first BZ with the irreducible path used in calculations assuming CoFeB and $\mu_0 H = 2$ T. Relevant parameters are given. (b) The first four magnonic bands for an ADL with $2R = 200$ nm. (c) Contours of constant frequency (isofrequency contours) of the first band from (b). (d) Magnonic band structure along the irreducible path in the first BZ for an ADL with $2R = 240$ nm.

arrays (section 2.2.1) and ADLs (section 2.2.2), with additional features characteristic of bi-component structures. In a 2D BMC with exchange-coupled materials, spin waves are subject to scattering on the interfaces between the two materials and exposed to a nonuniform demagnetizing field, the magnitude of which is proportional to the difference between the saturation magnetization values M_S of the constituent materials. Dipolar interaction between spin-wave modes localized in different segments of the BMCs is promoted via the intermediate ferromagnetic medium as well. Overall, in in-plane fields their SW band structures were found to be more involved compared to photonic crystals. This observation can be highlighted by referring to figure 5(d). Here, we approximate a BMC with a continuous ferromagnetic thin-film material that experiences (weak) periodic modulation. Then the empty lattice model (ELM) known, for example, from electronic band structures discussed in solid state physics textbooks serve as a starting point. Due to the anisotropic thin-film dispersion relations, back-folding by reciprocal lattice vectors **G** leads to many branches in the first BZ that cross. On the one hand this feature leads to numerous modes at the Γ point (figure 5(e)) that do not have an analogue in photonic crystals. On the other hand the opening of bandgaps at BZ boundaries is not straightforward, as many bands are found to overlap.

Still, 2D BMCs with sub-micrometer periodicity were shown to exhibit partial bandgaps [119]. Here, the demagnetizing field (not included in the ELM of figure 5(d)), periodic modulation of material parameters and Bragg diffraction were found to be relevant for the formation of the magnonic band structure. The demagnetizing field was responsible for frequency variations in the low-frequency part of the spectrum. The periodic modulation and the Bragg diffraction led to a splitting and hybridization of magnonic bands and to the opening of magnonic bandgaps, respectively. The main parameters that determined the width of the magnonic band gap were analyzed in the DE geometry. For a square-lattice BMC of lattice constant a these parameters were the filling fraction $\pi R^2/a^2$ and the difference between the magnetic parameters of the constituent materials, i.e. the contrasts in M_S and exchange lengths [119].

Edge modes localized at the boundary of the discs (inside the discs or in the surrounding material forming the matrix) can lead to similar properties to those observed in ADLs and arrays of separated discs. The modes depend on the materials used, their saturation magnetization values and the shape of the magnetic nanoelements [175]. Chessboard-like structures composed of squared Co and Py magnets have been investigated, too, not only from the perspective of magnonics, but also in terms of their phononic properties [176].

An attractive way for the fabrication of BMCs is by ion implantation of thin films, potentially covering large areas in a parallel exposure step [177, 178]. By this procedure the magnetization saturation [51] or magnetic anisotropy [179, 180] are changed in plain ferromagnetic films in periodic 1D and 2D patterns. At the macroscopic scale, ion implantation

in YIG was investigated already in the past [3, 177]. The magnetization contrast induced this way was sufficient to provoke reflection of spin waves incident at frequencies of the band gaps [181]. State-of-the-art nanopatterning techniques now allow similar studies at the nanoscale [51]. The implantation might influence the damping of SW, but this topic requires further investigation.

So far we have discussed bandgap properties. But thin-film 2D BMCs were investigated also for wave-guiding [118]. Studies based on micromagnetic simulations indicated that bi-component MCs can be more favorable for the filtering properties than antidot lattices or arrays of ferromagnetic discs, in that multiple broad bandgaps occurred [182]. Waveguides based on BMCs composed out of two metals such as Co, Ni, Py or Fe were optimized for large bandgaps by adjusting the filling fraction, shape of discs, bias magnetic field and lattice constants when exchange interaction predominated [46, 183].

2.3. 3D thin-film MCs

Thin-film MCs might experience an inhomogeneous magnetic configuration across the thickness. The corresponding spin dynamics have been studied in two classes of structures:

- Ferromagnetic films where a single or two surfaces are periodically corrugated (figure 3(b)) [35, 184–192]. Corrugation is assumed when the depth of the modulation is much smaller than the in-plane periodicity.
- Thin-film MCs with an inhomogeneity across the thickness comparable in size to the period of the MC [193].

The former class has already a long history of research, while studies of the latter are only at the initial stage [193]. An additional interaction between confined modes is introduced when an array of ferromagnetic discs is placed on top of a ferromagnet, or a disc array is covered by another ferromagnetic material [194] or a metal in which magnetization is induced [195]. The stray field of discs can be used also to introduce a periodically modulated magnetic field in a thin film. Thereby, one avoids directly embedding scattering centers but still creates periodic properties to modify the SW band structure [194]. According to the classification introduced in figure 2, such structures are 3D thin-film MCs, and the research on these structures has just started. This is an interesting part of magnonics with relations to other fields as well [196, 197]. It was shown that apart from both angular-dependent coercive fields and remanent magnetization values, the magneto-optical properties strongly depended on the composition across the thickness of 3D thin-film MCs.

The periodic modulation of the surface topography of a plain ferromagnetic film has been addressed earlier. Few microns thick films of YIG with one or two periodically corrugated surfaces were investigated theoretically [185] and experimentally [184] in the 1970s. Due to the thickness of the considered films and their periodicity (typically hundreds of micrometers) the magnetostatic interaction predominated over the exchange interaction, and the magnetostatic approximation was assumed in the theoretical studies. Bragg reflections and the opening of magnonic bandgaps for surface and volume magnetostatic waves were shown in [198–200] for sinusoidal-like modulation of the surface of a YIG film. Such structures have been considered, for example, as magnetostatic wave filters [35, 185–187]. YIG surfaces periodically grooved on various length scales (now with periodicities down to a few hundred nm) and with different geometries have been under investigation for a long time, substantiating good agreement between theoretical and experimental results [188–192, 201–206]. The control of the magnonic bandgap by adjusting structural parameters and by the external magnetic field is thus already well founded. The position of the magnonic bandgaps and the transmission properties depended on the SW propagation direction in a 1D array of grooves on YIG in [191]. Strong magnetic field anisotropy was shown as well [207]. The hybridization of magnetostatic waves propagating in the plane with quantized exchange waves confined between the top and bottom surfaces in differently thick segments was considered as a mechanism for bandgap opening in [208]. A theory of SW-based quasi-optics was developed for the external magnetic field oriented along the normal to the periodically modulated surface [209, 210]. Tailored spin-wave transmission through a defect state introduced into a 1D MC based on YIG was demonstrated recently in [211].

YIG films with thickness modulations periodic in two lateral directions have been considered theoretically and experimentally [212, 213]. Solutions of the Walker equation were found with simplifications regarding the excitation profile across the thickness. In [213] the finite difference method was implemented to model microstripe transmission measurements showing magnonic bandgaps. Studies on metallic films are rather rare [214]. In most cases the studies were devoted to magnetostatic spin waves with negligible effect of exchange interactions.

In the DE geometry, surface corrugation is expected to provoke nonreciprocal SW dispersions [215], similar to the metallization of the surface discussed in section 2.1.6. Metallization of a corrugated YIG surface should further enhance the nonreciprocity. Recent studies aim at the experimental verification of predicted Bragg resonances and magnonic bandgaps in samples in which the nonreciprocity is significant [110].

The Heisenberg model, extensively used in the calculations of SWs in thin films with a thickness ranging from a monolayer up to tens of monolayers, was extended to thin-film MCs with periodically corrugated surfaces. In [216] the Heisenberg model on a simple-cubic lattice with dipolar interactions was used for the calculation of a 20 nm thick permalloy film with one and two corrugated surfaces. Complex spectra were obtained with magnonic bands crossing within the BZ. These structures differ from the YIG samples described above in that the film thickness and periodicity-to-corrugation-depth ratio are much smaller. Nonreciprocal properties of SWs could have been expected, but were not addressed in [216].

Other topics investigated in 3D thin-film MCs include the influence of the periodicity on the relaxation of spin waves. Periodic surface corrugation was shown to increase the line width in FMR measurements at selected frequencies due to two-magnon scattering on a periodic lattice of defects [217]. The developed perturbation theory explained the observed frequency dependence of the extra damping in ferromagnets with periodically modified surface topography [218].

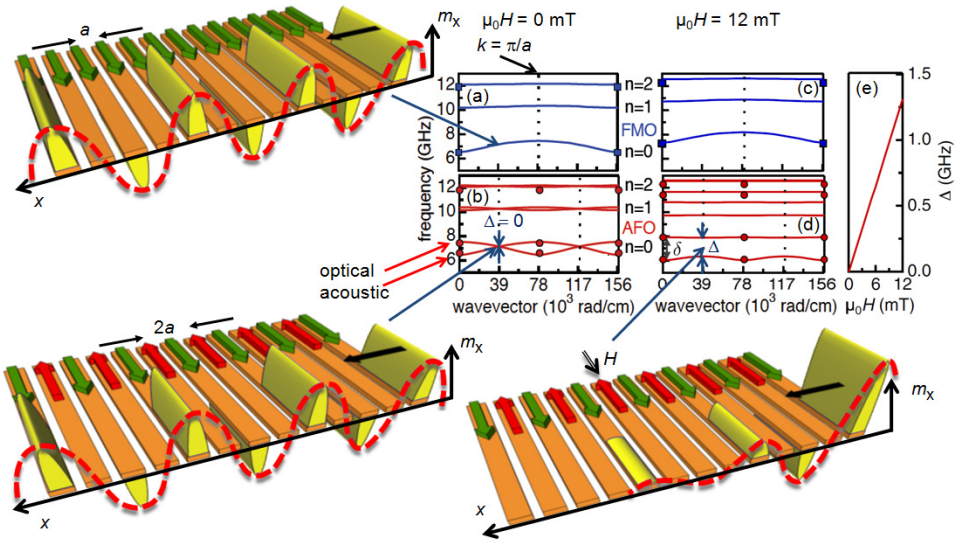

Figure 11. Band structures in (a) FMO and (b) AFO configurations at $H = 0$ as calculated for 300 nm wide Py stripes with $a = 400$ nm in [15]. In an applied field $\mu_0 H$ of 12 mT the branches are found to shift differently in (c) FMO and (d) AFO configurations. (e) Forbidden frequency gap Δ as a function of H for AFO. Theoretical curves (lines) and data (symbols) are taken from [15]. Spin-precessional amplitudes, i.e., the x-component of the dynamical magnetization (connected via dashed lines), are sketched for $\lambda = 4a$ at a given time. Bars indicate stripes, bold arrows denote the orientation of $\mathbf{M}$. δ refers to the splitting between the acoustic and optical modes for AFO, n is number of nodes in a stripe. Vertical dotted lines indicate BZ boundaries in reciprocal space. We depict the repeated zone scheme. Adapted from [15, 231].

3. Reprogrammable magnonic crystals

At remanence, a monodomain nanomagnet with uniaxial magnetic anisotropy has two energy minima for opposing orientations of the magnetization $\mathbf{M}$ collinear with the easy axis. The nanomagnet is bistable and the two different remanent states can be defined as 'zero' and 'one'. This property is useful for data storage and is under research for nanopatterned magnetic recording media. We stress here that such a magnetic property gives rise to reprogrammable magnonic band structures and dynamic responses. They are designed via different quasi-static magnetic states of subcomponents of an MC or magnonic device. Merely hysteretic dynamic response has been achieved in that, for example, magnetic-state dependent ferromagnetic resonance [21–23, 219–222], magnetic photonic crystal behavior [223] and standing spin waves were addressed [224–226]. In these works the authors did not elaborate on propagating spin waves and band structure formation. We are now interested in reprogrammable periodic structures consisting of interacting unit cells that give rise to collective SWs that follow Bloch's theorem and support propagation.

Programmable magnonic crystals could be understood in various ways. As outlined in section 2, the SW dispersion relations change by rotating a relatively small magnetic field with respect to high-symmetry directions of a thin-film MC. This feature by itself could be regarded as a programmable property of MCs that is not easily achieved in photonic or plasmonic artificial crystals. In this paper, however, we shall highlight MCs for which the magnetic configuration can be switched between different states, e.g. between ferromagnetic (FMO) and antiferromagnetic order (AFO) of subcomponents. Reprogrammable MCs are realized with unit cells that have at least two stable magnetic states. This can be reached with a unit cell composed of two subcomponents that exhibit, for example, different reversal fields and are switched independently from each other. Below we describe different approaches by which reprogrammable MCs were achieved and might be developed further in the future.

3.1. Reprogrammable 1D thin-film MCs

1D MCs with reprogrammable band structures have been realized by arrays of bistable ferromagnetic stripes. This approach is schematically shown in figure 11. General aspects of the band structure formation have been described above in section 2.1.1 for the saturated state, i.e., the FMO configuration. In [15] the reversal of selected stripes achieved in minor-loop measurements led to distinctly different resonance frequencies near $H = 0$. Characteristic resonances were observed that were attributed to a different periodic magnetic order, suggesting the AFO configuration. Theoretical calculations showed that the different dynamic response was consistent with a reprogrammed band structure for collective SWs (figure 11(a) and (b)). The modified magnetic unit cell consisted of two nanostripes with antiparallel magnetization $\mathbf{M}$ and was stable in the remanent state at $H = 0$. These findings coined the term 'reconfigurable artificial crystal'. MCs with a reprogrammable band structure now include periodic stripe arrays with unit cells incorporating two stripes of different widths or thicknesses [60, 66, 227], stripes with the same cross section but made of two different materials [83, 84, 228, 229] and stripes where every second one is directly attached to a reversal pad. The ferromagnetic pad launches domain walls at smaller H compared to the switching field of a bare stripe [60, 230]. These design

modifications compared to figure 3(a) allow one to achieve a high degree of magnetic ordering in both FMO and AFO.

Changes in the band structure that result from a switching of **M** in every second stripe of an MC have been discussed in [15, 231]. First we consider very long and identical stripes where the static dipolar coupling is assumed to be negligible. In the FMO configuration all the stripes in the MC are magnetized in the same direction (top row in figure 11). The unit cell includes a single stripe and an air gap, and the lattice constant is a. The boundary of the first BZ is found at π/a (figure 11(a)). In the AFO configuration (bottom row in figure 11) the lattice constant is $2a$ and twice as large since the unit cell includes two oppositely magnetized stripes. Thus, in reciprocal space, the BZ for AFO is half the size of the BZ for FMO. At the same time, the number of bands is doubled (figure 11(b)). For bands originating from the fundamental mode, acoustic and optical modes at $k = 0$ were indeed observed [15]. Note that at $H = 0$, AFO branches that appear to be back-folded from FMO branches by a reciprocal lattice vector of $2\pi/(2a)$ are not exactly at the FMO eigenfrequencies. The discrepancy arises from phase differences between out-of-plane components of the dynamic magnetization **m** of neighboring stripes belonging to AFO and FMO configurations [15]. These phase differences lead to a different dynamic dipolar coupling, thereby modifying slightly the eigenfrequencies of back-folded branches after switching the MC from FMO to AFO.

In the remanent AFO state, the acoustic and optical bands are found to be degenerate at the boundary of the first BZ. As soon as a bias magnetic field is applied along the long axis of the stripes, the bands shift for both FMO (figure 11(c)) and AFO (figure 11(d)). Importantly, the separation δ of acoustic and optical modes increases and a forbidden frequency gap Δ opens in the AFO state. A uniform bias magnetic field applied to stripes with **M** pointing in opposite directions causes a periodic distribution of Zeeman fields in the 1D MC. As a consequence, a bandgap Δ opens at the BZ boundary attributed to coherent Bragg reflection [231]. The frequencies of the acoustic and optical branches decrease and increase, respectively, with increasing intensity of the magnetic field, similarly to bulk antiferromagnets [27]. For the stripe array of [15], Δ at the BZ boundary has been found to increase linearly from zero with increasing H [15] as long as reversal is prevented (figure 11(e)). This peculiar bandgap variation allows a field-tunable notch filter for propagating SWs. A meander-type ferromagnetic nanostripe has been investigated as a reprogrammable MC that could be used as a logic gate [232].

Beyond bandgap material properties, 1D MCs have provided a yet unforeseen effective-medium property in the AFO state when excited by a microwave antenna in the long-wavelength limit [230]. In contrast to both the FMO state and natural magnetic materials, the AFO unit cell with compensating antiparallel **M** has allowed one to excite DE-type SWs with reciprocal characteristics. The reprogrammable metamaterial property is relevant for logic devices based on interfering SWs launched in different directions of a multiple-connected magnonic circuit. Long-wavelength DE-type SWs are favorable compared to BVMWs due to the large v_g.

In the structure described above the unit cell of the MC includes a single stripe in the FMO configuration, and two stripes in the AFO configuration, modifying the extension of the BZ. When the unit cell is composed of two different subunits (e.g. two different materials or two stripes of different cross section) the BZ extension is the same in both magnetic configurations. The band structure is thus changed in a different way when reprogramming takes place. An array of Py stripes of different width (330 and 900 nm) is considered in [66, 233]. Here, the magnetization reversal is a two-step process due to different shape anisotropies helping to produce FMO and AFO with high reliability. In zero bias magnetic field the magnonic band structure and the magnonic bandgaps in FMO and AFO almost coincide. Still, there is a remarkable difference in the intensities of the measured BLS signals. In the FMO state the most intense lines vary from BZ to BZ. As a general rule, the mode of node number n is the most intense one in the $n+$ first BZ [40]. The reason is that the BLS intensity is proportional to the value of the dynamic component of the magnetization vector averaged over the unit cell. In the center of the BZ the BLS intensity is purely proportional to the normal component of the magnetization. In the AFO state the magnetization precesses in opposite directions in neighboring stripes; hence, the in-plane and out-of-plane components of the magnetization vector precess in-phase and out-of-phase, respectively, for the acoustic mode, and vice versa for the optical mode. As a consequence, the BLS intensity of the acoustic mode residing at small frequency is smaller than that of the optical mode in AFO. In nonzero magnetic field the differences between the BLS intensities of the two modes become visible also in the band structure as the contribution of the in-plane component increases with increasing wavevector [234]. This explains the observed variation of the BLS signals across the Brillouin zones.

In bi-component MCs composed of two different ferromagnetic materials the stripes might have the same cross section. In this case, different saturation magnetization values or magnetic anisotropies provoke different switching fields. The different materials can be in direct contact or separated by a nonmagnetic dielectric (e.g., air or an oxide). In the former case exchange coupling might occur, whereas in the latter case there might be only magnetostatic coupling. A recent paper reports on the ferromagnetic resonance of bi-component stripes with weak dipolar coupling [229]. The modal analysis based on the calculation of the SW spectra for isolated stripes indicated that the impact of the exchange coupling was of minor nature. In other materials (such as exchange-spring systems) the exchange coupling can be strong and have a significant effect on the band structure.

We now comment on 1D MCs formed by short stripes as investigated in [227]. Here, different states such as FMO and AFO lead to different quasi-static stray fields modifying the static dipolar interaction between the stripes. As a consequence, internal fields H_{int} are different and provoke eigenfrequency shifts depending on the length of the stripes. For short stripes, FMO and AFO branches are expected to be much more offset with respect to each other compared to the band structures shown in figure 11.

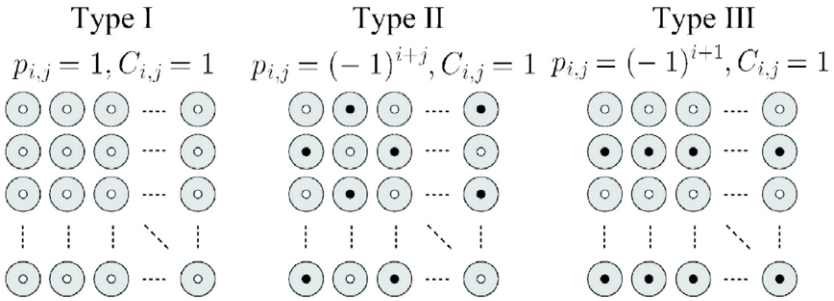

Figure 12. Three types of periodic lattices formed by different arrangements of vortex core polarizations p in a square array of nanodiscs as studied in [130]. White and black dots represent vortex core polarization, $p = 1$ and -1, respectively. $C_{i,j}$ denotes the chirality of the flux-closure configuration. $i\,(j)$ defines the row (column). Reprinted figure with permission from [130]. Copyright (2004) by the American Physical Society.

3.2. Reprogrammable 2D thin-film MCs

Reprogrammable 2D lattices of monodomain nanopillars have been considered recently [235, 236]. Assuming an initial state with out-of-plane magnetization (FMO) in the macrospin approximation, Verba *et al* predicted switching from the FMO to the true ground state under microwave irradiation. The ground state in zero field is a chessboard-like AFO configuration. The lattice allows band structure effects similar to those already discussed for 1D MCs. The magnetic reconfiguration converts the single-element unit cell into a larger bi-element one. Corresponding band structure modifications have been considered qualitatively in [131]. Note that collective SWs propagating in complex periodic arrays of single-domain nanopillars have been predicted to be nonreciprocal if two conditions are fulfilled [18]: (i) existence of a nonzero out-of-plane component of the pillars' static magnetization and (ii) a complex periodicity of the array's ground state with either at least two different nanopillars or at least three nanopillars per primitive cell if they are identical. State-of-the-art nanolithography thus allows one to tailor both the band structure and nonreciprocal wave properties. Such metamaterial property might give rise to integrated microwave circulators and isolators that do not require a bias magnetic field [18].

2D magnonic devices with reprogrammable band structures can be based also on arrays of coupled ferromagnetic discs in the vortex state (figures 8(a)–(c)). The vortex state is characterized by an up or down out-of-plane polarization p of the vortex core and a clockwise or counter-clockwise in-plane chirality C of the magnetic moments surrounding the core. The parameter p was predicted to modify the collective excitation spectra in a reconfigurable manner [130]. For square arrays of circular nanodiscs, analytical calculations showed that different arrangements of vortex core polarizations (figure 12) controlled the band structures formed by collective gyroscopic modes of coupled discs. In a lattice of random polarizations, localized modes were predicted to occur.

Interestingly, for 2D magnonic crystals one does not only modify the extension of the Brillouin zone and change k_{BZ} by switching to a new magnetic order, but one might rotate high-symmetry directions. Between Type I and Type II lattices in figure 12, the squared-shaped unit cell is rotated by 45°. Starting from a further Bravais lattice, one might arrive also at different lattice symmetries after switching appropriate nanomagnets. Combined linear chains and 2D arrays of nanodiscs exhibiting the vortex state (figures 8(c) and (d)) have been suggested to allow SW guiding and filtering in the low GHz frequency regime [79]. These considerations offer a so far unexplored playground for spin-wave control. It should be noted that the dynamic coupling is rather weak and a multi-element unit cell of a more complex architecture might be impractical for achieving reprogrammable band structures with appreciable miniband widths. The required close proximity or direct contact of discs in the array would in addition affect the stability of the static magnetic configurations.

The ideas developed for 1D thin-film BMCs have been transferred to 2D arrays with a bi-component unit cell in recent experiments and theoretical considerations [131, 237]. Stadium-like Py and Ni nanomagnets were fabricated in 2D lattices [228]. A stable antiparallel alignment of magnetization vectors was achieved in that the Ni nanomagnets switched at a smaller coercive field compared to the Py ones. The dipolar interaction between the two elements was adjusted via the edge-to-edge separation and controlled the switching [228]. In arrays with a small spacing between the elements the configurational anisotropy resulting from the static stray fields affected the switching fields as well.

The SW dynamics of pairs of elongated nanomagnets of Co and Py were investigated by time-resolved magneto-optical Kerr effect and micromagnetic simulations for different arrangements of the elements [238]. The dynamic response of binary component structures has already been shown to be useful for logic operations [228, 239]. Arrays with a three-component unit cell have been investigated recently as well [240], with the dynamic response measured by broadband FMR. Overall a large variety of elements could be created with the fabrication process outlined in [241], but so far the spectroscopy has addressed single elements. Band structures based on such kinds of reprogrammable unit cells still need to be explored.

Concluding this section, periodically patterned thin-film devices as sketched in the top row of figure 2 already serve as a powerful basis for a large variety of reconfigurable 1D and 2D MCs. From a technological point of view, the thin-film devices offer size reduction down to the nanometer scale, the integration with spintronic and/or semiconductor devices, and

low power consumption for manipulation of SWs. The scientific interests and challenges lie in (i) the anisotropic spin-wave dispersion relations [27, 28], (ii) the nonreciprocal properties of magnetostatic surface waves, (iii) the competition between dipolar and exchange interactions, and (iv) the inhomogeneous internal field, which can act as a potential barrier or confining well. Before we discuss further implications and perspectives in magnonics, we review research work done on bulk magnonic crystals. Note that current applications of ferromagnets in microwave technology, such as circulators and power limiters, require large power levels. Here thin-film-based magnonic devices might not be suitable.

4. Bulk magnonic crystals

From the theoretical side, bulk MCs were considered at an early stage. They served as a concept to get insight into the physical mechanisms leading to the formation of artificially tailored band structures for spin waves. The concept helped to set up simple and analytical models [242] by neglecting the effect of the external shape. Advantages of bulk MCs over thin-film MCs emerge in the field of metamaterials that are applied to electromagnetic (EM) waves in the microwave frequency regime. To modify the propagation characteristics of long-wavelength EM waves, individual thin films are insufficient but bulk samples are required. Bulk samples with periodically modulated properties are expected to interact with EM waves via their effective permeability. Bulk MCs can be useful also in sensing applications based on SW resonances [106], where positioning with micrometer precision is not required.

4.1. 1D bulk MCs: multilayers

Historically, multilayered thin-film structures (figure 2, bottom row on the left) can be viewed as the very first MCs that were investigated [243, 244]. A stack of different magnetic layers forms a 1D MC in the growth direction. The stack can be approximated by a bulk-like MC assuming a large lateral extent in the plane of the layers. When composed of magnetic and nonmagnetic layers such stacks gave rise to the discovery of the giant magnetoresistance (GMR) effect, as highlighted in [245]. The GMR effect was recognized with the Nobel prize in physics in 2007.

Multilayers of various compositions have been considered, i.e., two different ferromagnetic materials in direct contact or exchange-coupled by a metallic interlayer [246, 247], ferromagnetic films separated by nonmagnetic films [243, 248, 249], multilayers with anisotropic constituent materials [250] and multilayers composed of antiferromagnetic materials [251–253]. Modified magnonic bands have been found for surface or bulk waves, depending on the relative orientation of the SW wavevector with the external magnetic field and the direction of periodic modulation [242, 243, 249, 254, 255].

To understand the band formation in different regimes [256–259] the magnonic band structure was calculated in the magnetostatic approximation in [242, 248, 260, 261], neglecting the exchange interaction and retardation effects. For the exchange regime with dipolar interaction neglected, MCs were studied in [14, 262–266]. The theoretical predictions were addressed experimentally for magnetostatic modes [243, 267, 268] and in some special cases also for exchange-dominated waves [269]. In FMR studies the spectrum was shown to be formed by standing spin waves of discrete f with wavelengths matching the layer thicknesses [270]. Spin-wave resonances have been used recently for identifying the magnonic gap in multilayered 1D MCs [271].

A decisive role in the formation of magnonic bands is played by the strength of the dynamic coupling, which determines the band width and consequently the group velocity of the SWs propagating in the MC. The magnonic band structure has been shown to depend on the boundary conditions at the interfaces between the constituent materials of the multilayer and the interface profile between adjacent ferromagnetic films. A finite thickness of the interface region, an abrupt variation or continuous change of the magnetic parameters across the interface [272–278], as well as an interlayer exchange coupling were explored [275, 279]. The influence of SW damping on the magnonic band structure in 1D bulk MCs was studied in [280]. In this paper the effective damping was introduced and shown to depend on the SW frequency and the intensity of the external magnetic field. These studies were extended to 2D and 3D bulk MCs, as discussed in the next sections.

4.2. 2D bulk MCs

After the discovery of photonic crystals, first theoretical treatments of magnonic crystals regarded 2D lattices of infinitely long rods in a matrix (schematically shown in the center of the bottom row in figure 2) [281–283]. Under an external magnetic field applied along the rod axis and in the absence of anisotropy, the static internal magnetic field is uniform and equal to the external bias magnetic field. These conditions make the band structure of bulk 2D MCs qualitatively similar to corresponding photonic crystals. They have allowed one to study the effect of the arrangement and shape of the rods as SW scattering centers. The bandgap formation as well as the dependence of its width on the lattice type or cross-sectional geometry of the rods have thereby been investigated in detail. For a small lattice constant for which the exchange interaction determines the magnonic spectrum, SW scattering centers of the same symmetry as the lattice have been demonstrated to be the most favorable ones for the opening of bandgaps. For a given shape of scattering centers the magnonic gap proves to be the largest when the lattice has the largest coordination number [284]. Rotation of the rods around their long axis has been shown to provide a tool for tuning the magnonic bandgap in structures with rods of elliptical or square cross section [285, 286]. In [287] a strong anisotropy of the relaxation time has been found depending on the propagation direction of SWs with respect to the crystallographic axes. Directions with small SW damping and a relevant figure of merit have thereby been identified. The relevant formalism based on the plane-wave method has recently been extended to 3D bulk MCs, leading to the results discussed in the next section. Structural defects in 2D MCs induce localized resonances with frequencies in the band gap [288, 289]. They lead to wave-guiding channels and surface states.

4.3. 3D bulk MCs

3D bulk MCs (figure 2) would allow for the most comprehensive control of spin waves in all three spatial directions. Corresponding band structures have been studied only theoretically so far. In general, magnetic spheres in a 3D lattice interact via magnetostatic fields and a collective magnonic response is expected when their spacing is comparable to or smaller than the diameter of the spheres [290–293]. Research so far mainly focused on the FMR condition for collective precession of a lattice of interacting dipoles. Such structures are also proposed as metamaterials for electromagnetic waves [294–296].

In [255, 297–300] the roles of both structural and magnetic parameters were elucidated for band structure formation in 3D MCs. Parameters such as the filling fraction, lattice constant, ellipsoidal deformation of the scattering centers, contrast in saturation magnetization values and exchange constants of two constituent materials were explored using the plane-wave method. The lattices of the artificial crystals were considered to be simple-cubic (sc) [297], body-centered cubic (bcc) [255], face-centered cubic (fcc) [255] and simple hexagonal (sh) [299]. The magnetic parameters played a characteristic role for the opening of bandgaps. Increasing the saturation magnetization contrast above a critical value was sufficient to create a magnonic gap even if the values of the exchange constants were equal in the constituent materials. The critical value strongly depended on the lattice type. The exchange contrast had a significant effect on the bandgap width and needed to be very large to induce the opening of a magnonic bandgap in the case of identical saturation magnetization values. Though already the sc lattice was found to support magnonic band gap formation, the fcc lattice was optimum to create complete bandgaps [255]. Here, scattering centers being close to a sphere provoked the largest bandgap widths. The same was found for the bcc lattice. For lattice constants greater than the exchange length of the matrix material, the dipolar interaction gained in importance, leading to a substantial reduction of the bandgap width. The concept of a 3D bulk MC was used to explain the spin-wave frequency gap of low-doped manganites observed by neutron scattering [298, 301].

In [299] the theoretical considerations were extended to simple-cubic lattice based MCs composed of, in particular, two metallic ferromagnets. Twelve MCs of different composition (considering Co, Fe, Ni and Py) were explored. A complete magnonic bandgap was found to occur only for Ni spheres embedded in a Fe matrix. On one hand, the investigation highlighted difficulties when engineering 3D bulk MCs with complete bandgaps from conventional ferromagnetic metals. On the other hand, it is interesting that an sc lattice is sufficient to create complete magnonic bandgaps by appropriately choosing the magnetic materials. This is different from photonics, where a more complex diamond-like structure of dielectric materials is required to create complete bandgaps for light.

Different bottom-up and top-down techniques have yet been considered to fabricate 3D periodic lattices of magnetic unit cells. Self-assembly methods provide an opportunity for low-cost and large-scale fabrication of 3D bulk MCs. Among these methods, the protein crystallization technique of magnetoferritin seems to open the prospect of realizing 3D MCs with a lattice constant on the order of 10 nm [302, 303]. Here, fcc lattices consisting of ferrimagnetic Fe_3O_4 spheres with a diameter of about 8 nm were realized. The protein shell separating two neighboring nanomagnets was only a few nm thick, thereby allowing dipolar coupling between the magnetic cores. For temperatures below the blocking temperature, spectra showed a pronounced FMR line [304].

For all-magnetic MCs the protein matrix should be replaced by a ferromagnetic metal [305]. Such a structure would provide an enormous step forward in magnonics, as bandgaps in the sub-terahertz frequency regime would be possible. Considering the competition between exchange and dipolar interactions, the gap was found to be widest for a lattice constant of 13 nm for magnetoferritin nanoparticles with a diameter of 8 nm [306], i.e. close to the values already realized in magnetoferritin crystals [302, 303]. FMR measurements of the recently realized inverse-opal-like structures based on Ni [307] showed a complex dynamic response indicating collective modes. Besides the electrodeposition technique of [307, 308], atomic layer deposition of Ni [309, 310] might be useful to cover colloidal crystals of monodisperse polystyrene microspheres aiming at inverse opals. Even though there have not yet been reports of a magnonic bandgap, such structures seem to be promising for magnonics and magnetophotonics [311], as they support a photonic bandgap for electromagnetic waves.

5. Challenges and perspectives

In the following we discuss further challenges and perspectives in basic sciences and applied research when addressing MCs. Thereby we highlight some relevant aspects of figure 1. In the sections above, we did not consider damping in the SW dynamics in detail. It can however significantly modify the spectra. Ferromagnetic metals show a SW damping that leads to decay lengths of typically several 10 μm. In [312] spin-wave propagation in unpatterned Py was resolved over 80 μm. The role of damping is crucial when the SW propagation length is, for example, shorter than the width of the magnonic device. In that case the damping can affect the formation of eigenmodes, and thus the formation of the magnonic band structure [45]. Damping properties of nanostructured ferromagnets [313, 314] will be of primary importance if one thinks about integrated magnonic devices. Theoretical and experimental studies on anisotropic damping in both nanoelements [315] and nanopatterned MCs [159] are in their infancy. The effect of materials with different damping properties on both the relaxation time and decay length of SWs was considered theoretically for 3D MCs in [300]. A direct relation between the relaxation time of a mode and the distribution of its amplitude in the constituent materials was established. The relaxation time proved to be longer when the amplitude was concentrated more in the material with the smallest damping. The amplitude distribution in a given MC depends on the band number and the wavevector. This renders the relaxation time anisotropic.

Reconfigurable MCs and MCs with different degrees of disorder [316] would in particular be powerful to explore in

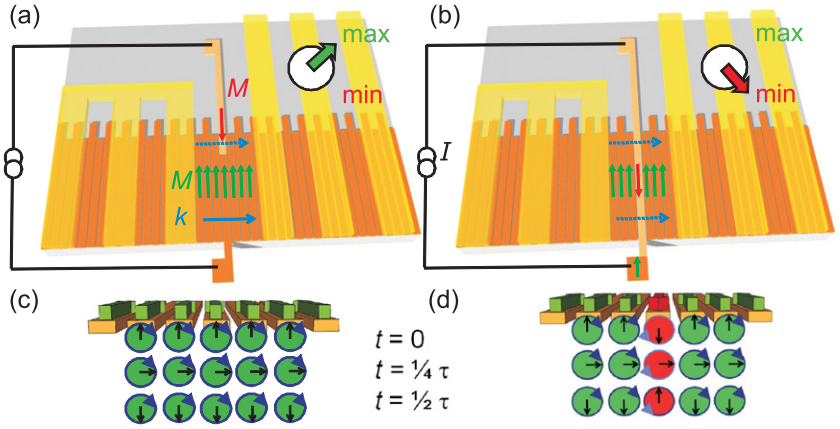

Figure 13. Sketch for spin-wave control on the nanoscale by reversing the magnetization of a single stripe in a 1D MC. (a) A stripe contains a domain wall at a position where only a small part of the SW is scattered (broken blue arrow). A large spin-wave signal (full blue arrow) is transmitted between the two neighboring CPWs (yellow). (b) Using a current, the domain wall has been moved such that the SW is largely scattered (broken blue arrows) and the detected SW signal is small. By reversing the current direction one can shift the domain wall back in the opposite direction, suggesting a transistor-like functionality. Using the spin-transfer torque effect from spintronics an integrated three-terminal device is thus possible where spin-wave control is achieved without applying a magnetic field. In (c) and (d) the precessional motion (indicated by arrows) of the dynamic component **m** is sketched for neighboring stripes at different times t within a period τ. For the illustration we assume a circular motion.

detail the effect of magnetic defects on the SW damping. Very recently it was shown experimentally and theoretically that an individual nanostripe of reversed magnetization provoked significant scattering of spin waves in an otherwise saturated 1D MC [317]. This is interesting for fundamental research but also for applications. The finding of [317] allows one to design a SW-based device that interconnects magnonics with spintronics. The concept is sketched in figure 13. In an array of ferromagnetic stripes being in the FMO state, one stripe is intentionally connected to a ferromagnetic pad by which a domain wall can be injected. The magnetization state of the single stripe is controllably reversed in that a domain wall is moved back and forth making use of the spin-transfer torque generated by an applied current I (figures 13(a) and (b)). As a consequence, the SW signal is varied between high and low levels. The reversed stripe undergoes a different sense of spin precession (figures 13(c) and (d)), thereby provoking SW scattering. As domain wall velocities can amount to about a few hundred m s^{-1} fast operation is possible. This 1D-MC-based three-terminal device is suitable for SW control on the nanoscale aiming at magnonic logic functionality. Magnetic defects in the AFO state offering reciprocal SW emission (see above) have not yet been explored in this framework.

A small decay length is in general a limiting factor for the application of waves as information carriers. Plasmonics (figure 1) deals with surface plasmon waves (polariton-plasmonic waves), i.e., collective excitations that couple electromagnetic waves and electron oscillations together and propagate along the surface of a metal. Plasmons could provide the basis for powerful manipulation of light at the nanoscale and integrated optoelectronic devices when using, for example, plasmonic crystals [318]. However, plasmonics as a technology faces the challenge on how to overcome metal losses impeding its progress [319]. For magnonics the discussion on losses and optimized materials is relevant as well. However, magnons exist in both metallic and insulating materials. The insulating ferrimagnet YIG provides a much larger decay and coherence length compared, for example, to metallic Py, as electronic intra- and interband excitations do not occur in the insulator[10]. Until very recently, high-quality YIG films required epitaxial growth on gadolinium gallium garnet using liquid phase epitaxy. The relevant thickness for low-damping material amounted to a micrometer or more. Such thick films are not an appropriate basis for the fabrication of magnonic nanostructures. Very recently, however, pulsed laser deposition allowed the preparation of low-damping YIG films with a thickness of only about 10–20 nm [323, 324]. The damping parameter was better by more than an order of magnitude compared to Py and further improvements might be expected in the future. Nanostructured devices and artificial crystals prepared from low-damping thin-film YIG are expected to further promote the field of magnonics. Making use of the spin Hall effect in a current-biased Pt overlayer, spin angular momentum injection into thick YIG was recently explored [325]. Such an approach has been argued to both overcome damping and provoke SW amplification [326]. The spintronics-based control of damping [327] promises intriguing perspectives of lossless wave manipulation on the nanoscale. Progress in magnonics might be less affected by damping issues compared to plasmonics.

For reprogrammable 1D MCs, micromagnetic simulations yielded overestimated values of the frequency splitting δ measured in the AFO configuration. Instead, an analytical model was used to achieve quantitative agreement with the experimental results [15, 72]. In this model a phenomenological parameter was introduced, referred to as a reduced dipolar coupling length. The role of the exact width, spacing and edge

[10] Discussions on microscopic sources for SW damping can be found, for example, in [320–322].

roughness [328–330] of the nanomagnets for the dipolar coupling has however not been fully elucidated yet; further studies are necessary, taking into account possible pinning mechanisms, inhomogeneities at the edges and the finite length of the stripes [60, 227]. Detailed analysis is necessary, as nanoscale physics goes beyond continuous models, and sophisticated measurements of local eigenfrequencies, damping characteristics [314] as well as phase differences between stripes are required. Special care is to be taken in the analysis of experimental and simulated data when the excitation of SW modes depends on the profile of the excitation field [230, 331–333].

Magnonic crystals with bistable stripes offer many more possible configurations than the FMO and AFO states that we have discussed so far [60, 316]. An MC with a total number of N stripes has 2^N different magnetic configurations. Also 2D MCs prepared from nanopillars with out-of-plane magnetization have many more magnetic configurations than discussed [334]. Not all of them will correspond to significantly different magnonic band structures, but the possibilities for defining states of different dynamic response are numerous. Experimental and theoretical studies on SWs in nanopatterned magnetic quasicrystals [335] or MCs based on aperiodic Fibonacci sequences [336–338] have been started. In plasmonics, aperiodic order has been explored to achieve localization of wave-like excitations and provoke near-field enhancement effects [339]. In magnonics, quasicrystals have been operated in an active ring resonator for eigenmode selection and dissipative soliton self-generation [338].

SW resonators positioned close to a periodically patterned waveguide (next to the waveguide or above it) seem to be an interesting approach for further tailoring the transmission properties as well. Preliminary results for a 1D magnonic structure have been presented in [94]. The approach, already well developed in photonics, is so far almost unexplored in magnonics. The prospects for new physics seem to be broad considering, for example, resonant coupling (where one expects a Fano-type resonance between propagating SWs and the resonator) which is promoted by either the dynamic stray field or the exchange coupling if the additional resonator is attached directly to the MC-based waveguide. The coupling might depend crucially on the magnetization direction of the SW resonator [340] thereby allowing reprogrammable characteristics.

In figure 10(c) we showed isofrequency contours in the FVMW geometry obtained in a 2D antidot lattice with out-of-plane magnetization. The different contours in the first BZ and the characteristic changes in their curvatures are consistent with photonic and phononic crystals that were shown to exhibit a negative refractive index [20, 341, 342]. The magnetic antidot lattices thus encourage the design of metamaterials with left-handedness for SWs. This research direction promises further discoveries in magnonics when using nanostructured ferromagnetic devices with and without reprogrammable characteristics. The FVMW geometry is expected to become more and more relevant for future MCs when magnetization vectors would be controlled in the out-of-plane direction, for example, via materials with perpendicular magnetic anisotropy [343, 344] or magnetostrictive/multiferroic approaches [345, 346].

An important issue for magnonic applications and integrated circuits is the injection of a SW packet from an emitter region into a magnonic waveguide or MC. The injection was already studied for a YIG-based 1D MC with modulated thickness [203] and a Py magnetic antidot lattice [347]. However, theoretical and experimental studies on the scattering of SWs from the border of MCs need further consideration.

In the previous sections we have limited ourselves to spin-wave excitations in the linear regime. Further challenges and research opportunities appear when nonlinear magnetization dynamics at large signal levels or interactions of SWs with other excitations in periodic structures are considered.

5.1. Nonlinear effects

Nonlinear aspects of magnetization dynamics in periodic structures are an important issue and provoke interesting physics [348, 349]. The theory was developed early [350–354] but interest in the subject has revived recently. Studies indicated that Bragg scattering in MCs is relevant for SW soliton formation. A soliton is a spatially localized wavepacket traveling with constant speed and shape. It preserves its character during interaction with other solitons. Solitons require a balance between dispersive properties and the nonlinearity of the medium. In photonics, solitons have been explored in great detail in glass fibers and photonic crystals for fundamental research and applications such as low-loss data transmission [355, 356].

Solitons from spin waves are an intriguing object for research as the SW dispersion relations in thin ferromagnetic films vary significantly with the direction and intensity of the external magnetic field. MCs offer even more possibilities for tailoring the conditions for soliton formation [351]. Bright and dark SW solitons were indeed observed in an MC consisting of periodic metallic stripes on a plain film of YIG [357, 358]. The solitons were generated at frequencies within the magnonic bandgap of the MC, which showed the vital importance of the proper shape of the magnonic band structure for their generation. Their significant sensitivity also to finite-size effects and relaxation of SWs indicates the need for studies on such effects in MCs. Signal-to-noise enhancement of SWs, suppression of high-power SW signals and power-dependent phase shifts have been observed in MCs [192, 348, 359, 360]. Solitons have been investigated also in MCs formed by an array of grooves in YIG [338, 361]. SW solitons in reprogrammable MCs are still to be explored and their functionality for lossless data transmission needs to be elucidated.

5.2. Cross-field applications of magnonic crystals

Possible cross-field applications of MCs involve magneto-elastic, magnetophotonic and magnetoplasmonic interactions. Studies on magnetoelastic interactions are numerous as these have been investigated in uniform ferromagnetic films for decades [362, 363]. Magnetophotonics was developed as a field studying the propagation of electromagnetic waves influenced by static magnetic properties. The latest field of research, magnetoplasmonics, combines magnetic properties with the propagation of surface plasmons [364, 365]. The

combination of SWs with other wave-like excitations in periodic structures is expected to enhance the tunability and functionality of artificial crystals.

5.2.1. Magnonic and phononic degrees of freedom. Magnonic and phononic spectra can have the same frequency range and similar wavevectors. Due to magnetoelastic coupling, collective magnetoelastic excitations can propagate in ferromagnetic films [362, 363, 366, 367]. Excitations at frequencies of up to a few gigahertz in films of micrometer thickness have been investigated. Magnetoelastic coupling can occur in all the geometries typically used in magnonics, i.e. the DE, BVMW and FVMW geometries [368, 369]. Magnetoelastic coupling in thin films of nanoscale thickness can effectively change the spin-wave dispersion and attenuate or excite spin waves [370–372]. The magnetoelastic coupling can also be used for energy conversion from phonons to spin waves [373–376]. As magnetoelastic waves are influenced by the substrate and overlayers [377] a large spectrum of parameters is provided for wave control.

The magnetoelastic interaction occurs in periodic structures as well. The magnetoelastic properties of multilayer structures were investigated in [378, 379]. In magnonic crystals this interaction and the related collective effects can be exploited for technological applications. The occurrence of magnonic and phononic bandgaps (in the DE geometry and for Rayleigh waves, respectively) in the same periodic structure was demonstrated in BLS measurements and supported by finite element calculations for both an array of Py stripes with dielectric spacing [380] and bi-component MCs composed of Fe (Ni) and Py stripes [82]. However, the coupling between the two dynamic subsystems has not been considered. A modification of the internal magnetic field by magnetostriction or reorientation transition was shown in plane-wave-method calculations [381]. As standing surface acoustic waves (SAWs) could be used for periodic modulation of the internal magnetic field the creation of dynamic magnonic crystals is possible [382, 383]. SAW-based control has been well developed in acousto-optic devices and is now being transferred to magnonics, where however it requires experimental investigation.

5.2.2. Magnonics and photonics. Photonic crystals made of magnetic materials are referred to as magnetophotonic crystals. Static properties of magnetic materials are used in these structures to provide new phenomena and photonic applications [384–386]. Magnetophotonic crystals can include MCs as components, but their magnetization dynamics hardly interact with terahertz electromagnetic fields due to wavevector mismatch between spin waves and electromagnetic radiation of the same frequency. Diffraction of electromagnetic waves at GHz frequencies on standing magnetostatic spin waves was studied theoretically and demonstrated experimentally in the 1970s [387–391]. The diffraction was observed in films in all three geometries, i.e. the DE [389], BVMW [390] and FVMW [392] geometries. To the best of our knowledge, there are no publications addressing periodic structures.

The missing link for the integration of photonics and magnonics might be provided by plasmonics combined with magnetic materials [393]. The structure and constituent materials of plasmonic crystals [318] can be matched with those used in magnonics, giving rise to magnetoplasmonics [364, 365, 394]. Plasmonic crystals require a similar scale of periodicity. Magnonic bandgaps can occur simultaneously with bandgaps for surface plasmons, though in a different frequency regime [395–397]. Recent theoretical studies indicate that magnonic and plasmonic excitations can be integrated in metal-ferromagnetic dielectric structures, to provide a basis for their interaction and further exploration of magnetoplasmonic periodic structures for technological applications [398]. This research direction is at a very early stage but intriguing functionalities might be expected from hybrid materials: (i) plasmonic nanostructures on ferromagnetic or multiferroic materials might enhance photon–magnon coupling for inelastic light scattering and photo-magnonics [32], and (ii) magnetization dynamics in ferromagnets might modify plasmons at ultra-short timescales via magnetoplasmonic effects [399]. One could speculate about ultrafast magnetic control of photonics.

Recently, thin-film MCs have been proposed as basic elements of metamaterials that manipulate electromagnetic waves from gigahertz to sub-terahertz frequencies [400–402]. Here, spin-wave resonances were proposed to provoke negative permeability. This, together with the metallic properties of the ferromagnetic material, guarantees a negative effective refractive index. Two mechanisms were used to increase the spin-wave resonance frequencies to sub-terahertz values: pinning of the magnetization dynamics on the film surface [400] and lateral quantization of spin waves by an MC [401].

5.2.3. Electric currents in magnonic crystals. Currents applied directly to a ferromagnetic device have the potential to modify the spin-wave spectrum. In heterostructures composed of uniform ferromagnetic, semiconductor and metallic films the interaction of unpolarized electric currents with spin waves was studied in the magnetostatic part of the spectrum and the possibility for spin-wave amplification was predicted [403–408]. Corresponding experimental data presented in [409] are however under discussion [27].

Recently, the interaction between spin-polarized currents and spin waves has been explored [410–414]. The Doppler effect for spin waves was demonstrated in micrometer-wide SW wave guides [410]. For an MC, the Doppler effect was predicted to shift the frequency spectrum [415].

5.2.4. Periodic lattices of skyrmions and domains. Magnetic materials with a non-centrosymmetric crystal lattice have attracted enormous attention in recent years [416–418]. Here, electronic correlations give rise to a rich magnetic phase diagram, showing phases such as helical, conical and ferromagnetic order as a function of temperature T and magnetic field H. The A-phase of chiral magnets has recently been found to consist of a 2D periodic lattice of skyrmions [416]. Skyrmions are vortex-like magnetic structures (cf figure 8(a)) where microscopic magnetic moments follow a twisted configuration [419]. They form hexagonal lattices in a self-organized manner due to a hierarchy of different magnetic energies,

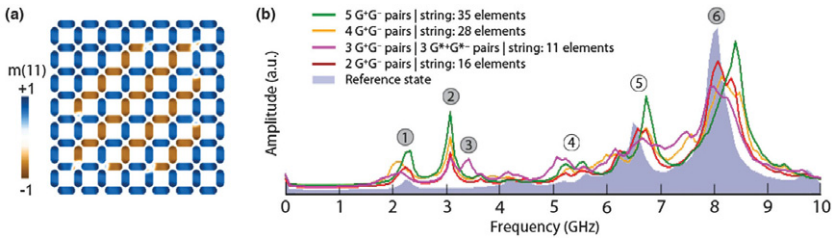

Figure 14. (a) Simulated lattice composed of 112 stadium-like Py magnets forming artificial square spin ice. It contains topological defects, i.e., four $G^{+}G^{-}$ pairs connected by strings extending over 28 elements. $G^{\pm}$ ($G^{*\pm}$) denote magnetic charges of ± 1 (± 2) at a vertex. (b) Magnetization dynamics spectrum for different numbers of magnetically charged vertices and different string lengths compared to the saturated reference state. The shaded labels indicate signatures of the topological defects. The amplitude units are identical in all cases. Reprinted figure with permission from [459]. Copyright (2013) by the American Physical Society.

such as exchange, Zeeman and magnetocrystalline anisotropy energies as well as the Dzyaloshinskii–Moriya interaction. The skyrmion lattices have been evidenced in different materials such as magnetic metals, semiconductors and insulators [416–418]. They have been identified in bulk and thin-film materials in different regimes of magnetic field and temperature, even close to room temperature [420].

The periodic modulation of the magnetic properties provoked by the skyrmion lattice is expected to specifically tailor the magnonic band structure. Lattice constants of 2D skyrmion arrays are on a length scale of a few tens of nm, not easily achieved by standard top-down nanolithography. Intriguingly, currents [421, 422] and electric fields [423] have both been shown to modify the properties of the 2D periodic skyrmion lattices, suggesting current- and electric-field controlled magnonics. Experimental and theoretical studies on the spin dynamics and damping are however at an initial stage [424–430] and the potential of the skyrmion phase for spintronics and magnonics still needs to be explored. Very recently, a method has been presented how to produce artificial 2D skyrmion crystals by making use of nanotechnology [431]. Such approaches will certainly fuel further research activities on functionalities offered by these periodic spin textures.

Periodic magnetic patterns in one and two dimensions can be formed in continuous films also by magnetic domains. Due to competition between exchange, magnetostatic and magnetic anisotropy energies, regular arrays of stripe or bubble domains can minimize the total energy of the ferromagnet. In the 1970s bubble domains were regarded promising for computer memory, data processing and optical image processing [432–434]. Numerous theoretical [435–437] and experimental studies [434, 438–441] on magnetization dynamics have already been conducted, but the application in magnetic memory devices [442] was not sustainable. Now, with growing interest in magnonics, these periodic lattices of magnetic domains might be revisited [443]. In some kind of self-organization process the patterns are formed spontaneously and possess reconfigurable properties [444]. In thin films containing stripe domains, SW excitation spectra are complex, as nonuniform internal fields are relevant and domain wall oscillations in the low GHz frequency regime contribute to the spectra [445–450]. Still, the ferromagnetic material is homogeneous. In particular, air gaps (compare figure 3(a)) are avoided such that truly exchange-dominated spin waves might be tailored by the periodic magnetic modulation and experience magnonic crystal behavior. A magnetic field or spin-polarized currents could be used to shift domain walls and thereby control the SW properties.

5.2.5. Artificial spin ice and artificial ferroics. Monodomain nanomagnets periodically arranged on a 2D lattice (figure 14(a)) have been shown to reflect frustration effects from competing dipolar interactions [451]. Arranged in specific lattices, nanomagnets cannot minimize all interaction energies at the same time, leading to degeneracy of low-energy states and frustration. So far, mainly the quasi-static properties of these so-called artificial spin ice (ASI) systems have been investigated while searching for both the ground-state configuration [452] and characteristic topological defects [453]. It was already argued [453] that the ASI research field has a natural connection to magnonics, as the exploration of magnetic excitations will be especially important to understand the thermal dynamics [454–456]. Beyond this, we believe that ASI is intriguing for magnonics in that it forms a specific and very interesting subgroup of reconfigurable magnonic crystals. To our knowledge, experiments and simulations on SW modes are very few so far. But a broadband ferromagnetic resonance experiment [457] together with simulation results (figure 14) [458, 459] has already suggested that characteristic magnonic modes exist that reflect ground-state and topological-defect properties. The artificial square spin ice of [451] is the archetypical ASI configuration. Later, ASI physics has been studied also in, for example, antidot lattices [460] and connected honeycomb structures [454], sometimes called artificial kagome spin ice.

The intriguing perspectives of ASI are provided by the large variety of magnetic configurations that are possible depending on the magnetic field and thermal history [461]. The change of a geometrical structure in spin ice systems leads also to non-trivial configurational dynamics [460, 462]. Once the formation of the different magnetic configurations and defect states is understood in detail, ASI might be functionalized in magnonics to reconfigure SW band structures and support propagating SWs. One can imagine defect lines serving as channels of nanoscale width for guiding SWs [459] or specific domain boundaries [461], modifying both SW transmission coefficients and SW phases across the ASI. The variety of

magnetic states that are controlled globally via a specific magnetic field history goes beyond the MCs discussed and explored so far.

The magnetoelectric compound $BiFeO_3$ has recently been shown to provide electric-field control of SW resonances [463]. Artificially tailored structures based on multiferroic components give another advantage for MCs, especially in terms of their reprogrammable properties. Multiferroic heterostructures are composed of interacting ferroic components such as ferromagnetic and ferroelectric layers, thereby providing numerous opportunities for designing artificial structures and functionalities [452]. Electric-field control of magnetism in multiferroic heterostructures has been considered for applications such as sensors, transducers, filters, oscillators, logic and information storage devices [464, 465]. At the same time, SW frequencies can be controlled in combined ferromagnetic and ferroelectric layers via, for example, an electric-field dependent magnetic surface anisotropy or strain [466, 467]. MCs based on multiferroic components are expected to provide energy efficient means for reconfiguration of SW properties by avoiding currents for magnetic field generation. Low power consumption is a key for integrated magnonic circuits aiming at microwave and signal processing at GHz frequencies [31].

5.2.6. Topological magnonic crystals. Another promising direction of research is related to the recently introduced topological magnon insulator [468] and the discovery of the magnon Hall effect [469, 470]. Periodically patterned ferromagnets can be used for designing so-called topological magnonic crystals [471, 472]. The research in this direction has just started, but it seems to be rich in new physics. In specifically designed MCs, magnetostatic spin waves might be realized that form protected chiral edge modes that are qualitatively similar to protected edges states in electronic topological insulators. In these edge modes, spin waves propagate in a unidirectional way without being scattered backward [471]. Reprogrammable characteristics of MCs due to different remanent states are unexplored in this field.

5.2.7. Spin-wave transistors based on MCs. Based on figure 13 we discussed an approach for a three-terminal transistor-like SW device based on a 1D MC. Here, a spin-polarized current was argued to control the SW response. However, for all-magnon-based logic one aims at control by spin waves. A three-terminal magnon transistor has recently been presented by Chumak *et al*. They considered a 1D MC with three integrated microwave antennas. The central antenna modified the magnon population within the MC and thereby controlled the SW transmission properties [473]. Understanding the microscopic mechanisms and efficiency for SW control in detail would allow the design of all-magnon-based logic using integrated magnonic circuits. Such an approach might be further combined with frequency conversion and SW front reversal evidenced in dynamically controlled MCs [54], leading to unexplored possibilities for integrated magnonic circuits with reconfigurable properties.

5.2.8. Grating coupler and spin-wave focussing. Periodic lattices open the perspective of efficient microwave-to-magnon transducers covering a broad range of SW wavevectors. Considering a periodic grating from nonmagnetic silver between a microwave antenna and ferromagnetic thin film, the idea of converting a microwave field into spin waves was realized in [474]. However, the uniform spin-precessional mode with wavevector $k = 2\pi/\lambda = 0$ was pronounced, and partly obscured spin waves of shorter wavelength exhibiting a small signal strength. Recently, periodically patterned thin-film ferromagnets underneath a CPW were used to emit short-wavelength SWs in many different in-plane directions just depending on the lattice symmetry [475]. This so-called magnonic grating coupler can be optimized further when (i) using magnetic scatterers that undergo resonant spin-precessional motion [476] and (ii) combining different Bravais lattices underneath a CPW. For in-plane fields, extra damping by magnon scattering is expected for selected frequencies when reciprocal lattice vectors connect dispersion relations in different spatial directions [218]. For out-of-plane fields, extra damping might be less effective due to the isotropic dispersion relations of FVMWs [477]. However, this needs to be explored. In plasmonics, specifically tailored grating couplers led to wavefront engineering of, for example, plasmon focussing devices [478]. In magnonics, similar achievements are expected [474]. Here, different magnetic states might open novel perspectives, in that grating couplers and magnon focussing devices become reprogrammable.

6. Summary

We have provided an overview on artificial crystals offering tailored band structures for spin waves. Compared to other periodic structures, such as photonic, phononic or plasmonic crystals, the fabrication and measurements of magnonic crystals provide more challenges because of the anisotropy of spin-wave dispersion relations and the different local and nonlocal interaction effects between spins. At the same time, the complex interplay between SW properties, geometrical shape and magnetic configurations gives rise to a fascinating new area of research on wave phenomena in solids. The research reaches from the microwave signal processing already addressed in the early 1970s to the recently suggested topological magnonic crystal.

We have highlighted the reconfigurable artificial crystals as a further intriguing objective. Combined, for example, with piezoelectric materials or multiferroic heterostructures, magnonic crystals offer unprecedented spin-wave control. Miniaturization down to the nanometer scale and operating frequencies up to the sub-terahertz regime make magnonic crystals attractive for signal processing and wireless telecommunication. Considering the significant improvement in the SW damping of thin YIG films in recent years, magnonics as an emerging nanotechnology might face less discussions concerning damping issues, as has been the case for plasmonics. In fact, magnonics could fill the gap between electronics, spintronics and photonics, concerning speed and integration feasibilities. To achieve this, further elements need to be investigated and

developed, including efficient SW sources and detectors. Here, interconnections of magnonics with spintronics, plasmonics and photonics will be of special relevance. To define the benefits of magnonic crystals in microwave applications, such as circulators and limiters subject to high power levels, further research efforts are required. Considering the manifold interconnections of magnonics with further research disciplines and technologies, interesting physics and discoveries are to be expected for the future manipulation of waves in solids.

Acknowledgments

We thank D Heitmann, M Kostylev and J Topp for support and H Yu for providing sketches. Research topics entering this review have received funding from the European Community's Seventh Framework Programme (Grant No. FP7/2007–2013) under Grant Agreements No. 247556 (People)–NoWaPhen and No. 228673–MAGNONICS project. Partial support was provided also by NCN of Poland project DEC-2-12/07/E/ST3/00538, the DFG via the German excellence cluster 'Nanosystems Initiative Munich', project GR1640/5-1 of the priority programme 'Spin Caloric Transport' SPP1538, and the Transregio/SFB TRR80 'From electronic correlations to functionality'.

References

[1] Elachi C 1976 *Proc. IEEE* **64** 1666
[2] Owens J M J, Smith C, Lee S and Collins J 1978 *IEEE Trans. Magn.* **14** 820
[3] Volluet G 1981 *IEEE Trans. Magn.* **17** 2964
[4] Demidov V E, Demokritov S O, Rott K, Krzysteczko P and Reiss G 2008 *Appl. Phys. Lett.* **92** 232503
[5] Duerr G, Thurner K, Topp J, Huber R and Grundler D 2012 *Phys. Rev. Lett.* **108** 227202
[6] Tacchi S *et al* 2012 *Phys. Rev.* B **86** 014417
[7] Yablonovitch E 1987 *Phys. Rev. Lett.* **58** 2059
[8] John S 1987 *Phys. Rev. Lett.* **58** 2486
[9] John S 2012 *Nature Mater.* **11** 997
[10] Tsakmakidis K and Yablonovitch E 2012 *Nature Mater.* **11** 1000
[11] Pendry J B 2000 *Phys. Rev. Lett.* **85** 3966
[12] Ziolkowski R W 2004 *Phys. Rev.* E **70** 046608
[13] Yanik M F and Fan S 2004 *Phys. Rev. Lett.* **92** 083901
[14] Dobrzynski L, Djafari-Rouhani B and Puszkarski H 1986 *Phys. Rev.* B **33** 3251
[15] Topp J, Heitmann D, Kostylev M P and Grundler D 2010 *Phys. Rev. Lett.* **104** 207205
[16] Zheludev N I and Kivshar Y S 2012 *Nature Mater.* **11** 917
[17] Khitun A 2012 Energy dissipation in magnonic logic circuits *IEEE-NANO: 12th IEEE Int. Conf. on Nanotechnology*
[18] Verba R, Tiberkevich V, Bankowski E, Meitzler T, Melkov G and Slavin A 2013 *Appl. Phys. Lett.* **103** 082407
[19] Engheta N and Ziolkowski R W 2006 *Metamaterials: Physics and Engineering Explorations* (New York: Wiley–IEEE)
[20] Joannopoulos J D, Johnson S G, Winn J N and Meade R D 2008 *Photonic Crystals: Molding the Flow of Light* 2nd edn (Princeton, NJ: Princeton University Press)
[21] Encinas A, Vila L, Darques M, George J M and Piraux L 2007 *Nanotechnology* **18** 065705
[22] Kou X, Fan X, Zhu H and Xiao J Q 2009 *Appl. Phys. Lett.* **94** 112509
[23] Medina J D L T, Piraux L and Encinas A 2010 *Appl. Phys. Lett.* **96** 042504
[24] Akhiezer A I, Bar'yakhtar V G and Peletminskii S V 1968 *Spin Waves* (Amsterdam: North-Holland)
[25] Kalinikos B A and Slavin A N 1986 *J. Phys. C: Solid State Phys.* **19** 7013
[26] Kabos P and Stalmachov V S 1994 *Magnetostatic Waves and their Applications* (New York: Chapman and Hall and Ister Science Press)
[27] Gurevich A and Melkov G 1996 *Magnetization Oscillations and Waves* (Boca Raton, FL: CRC Press)
[28] Stancil D D and Prabhakar A 2009 *Spin Waves. Theory and Applications* (Berlin: Springer)
[29] Kruglyak V V, Demokritov S O and Grundler D 2010 *J. Phys. D: Appl. Phys.* **43** 264001
[30] Serga A A, Chumak A V and Hillebrands B 2010 *J. Phys. D: Appl. Phys.* **43** 264002
[31] Khitun A, Bao M and Wang K L 2010 *J. Phys. D: Appl. Phys.* **43** 264005
[32] Lenk B, Ulrichs H, Garbs F and Münzenberg M 2011 *Phys. Rep.* **507** 107
[33] Demokritov S O and Slavin A N (ed) 2013 *Magnonics from Fundamentals to Applications* (Berlin: Springer)
[34] Khitun A 2012 *J. Appl. Phys.* **111** 054307
[35] Hartemann P 1984 *IEEE Trans. Magn.* **20** 1272
[36] Neusser S and Grundler D 2009 *Adv. Mater.* **21** 2927
[37] Gubbiotti G, Tacchi S, Madami M, Carlotti G, Adeyeye A O and Kostylev M 2010 *J. Phys. D: Appl. Phys.* **43** 264003
[38] Krawczyk M, Mamica S, Mruczkiewicz M, Klos J W, Tacchi S, Madami M, Gubbiotti G, Duerr G and Grundler D 2013 *J. Phys. D: Appl. Phys.* **46** 495003
[39] Gubbiotti G, Tacchi S, Carlotti G, Singh N, Goolaup S, Adeyeye A O and Kostylev M 2007 *Appl. Phys. Lett.* **90** 092503
[40] Kostylev M P and Stashkevich A A 2010 *Phys. Rev.* B **81** 054418
[41] Gubbiotti G, Tacchi S, Carlotti G, Vavassori P, Singh N, Goolaup S, Adeyeye A O, Stashkevich A and Kostylev M 2005 *Phys. Rev.* B **72** 224413
[42] Kostylev M, Schrader P, Stamps R L, Gubbiotti G, Carlotti G, Adeyeye A O, Goolaup S and Singh N 2008 *Appl. Phys. Lett.* **92** 132504
[43] Zivieri R, Montoncello F, Giovannini L, Nizzoli F, Tacchi S, Madami M, Gubbiotti G, Carlotti G and Adeyeye A 2011 *IEEE Trans. Magn.* **47** 1563
[44] Nguyen H T and Cottam M G 2011 *J. Phys. D: Appl. Phys.* **44** 315001
[45] Mruczkiewicz M, Krawczyk M, Sakharov V K, Khivintsev Y V, Filimonov Y A and Nikitov S A 2013 *J. Appl. Phys.* **113** 093908
[46] Ma F S, Lim H S, Wang Z K, Piramanayagam S N, Ng S C and Kuok M H 2011 *Appl. Phys. Lett.* **98** 153107
[47] Ma F S, Lim H S, Zhang V L, Wang Z K, Piramanayagam S N, Ng S C and Kuok M H 2012 *J. Appl. Phys.* **111** 064326
[48] Wang Z K, Zhang V L, Lim H S, Ng S C, Kuok M H, Jain S and Adeyeye A O 2009 *Appl. Phys. Lett.* **94** 083112
[49] Wang Z K, Zhang V L, Lim H S, Ng S C, Kuok M H, Jain S and Adeyeye A O 2010 *ACS Nano* **4** 643
[50] Polushkin N I, Michalski S A, Yue L and Kirby R D 2006 *Phys. Rev. Lett.* **97** 256401

[51] Obry B, Pirro P, Bracher T, Chumak A V, Osten J, Ciubotaru F, Serga A A, Fassbender J and Hillebrands B 2013 *Appl. Phys. Lett.* **102** 202403

[52] Popkov A F, Fetisov Y K and Ostrovskii N V 1998 *Tech. Phys.* **43** 576

[53] Chumak A V, Neumann T, Serga A A, Hillebrands B and Kostylev M P 2009 *J. Phys. D: Appl. Phys.* **42** 205005

[54] Karenowska A D, Gregg J F, Tiberkevich V S, Slavin A N, Chumak A V, Serga A A and Hillebrands B 2012 *Phys. Rev. Lett.* **108** 015505

[55] Bai L, Kohda M and Nitta J 2011 *Appl. Phys. Lett.* **98** 17258

[56] Ding J, Jain S and Adeyeye A O 2011 *J. Appl. Phys.* **109** 07D301

[57] Zivieri R, Montoncello F, Giovannini L, Nizzoli F, Tacchi S, Madami M, Gubbiotti G, Carlotti G and Adeyeye A O 2011 *Phys. Rev.* B **83** 054431

[58] Xing X, Li S, Huang X and Wang Z 2013 *AIP Adv.* **3** 032144

[59] Ciubotaru F, Chumak A V, Grigoryeva N Y, Serga A A and Hillebrands B 2012 *J. Phys. D: Appl. Phys.* **45** 255002

[60] Topp J, Mendach S, Heitmann D, Kostylev M and Grundler D 2011 *Phys. Rev.* B **84** 214413

[61] Mathieu C *et al* 1998 *Phys. Rev. Lett.* **81** 3968

[62] Jorzick J, Demokritov S O, Mathieu C, Hillebrands B, Bartenlian B, Chappert C, Rousseaux F and Slavin A N 1999 *Phys. Rev.* B **60** 15194

[63] Guslienko K Y, Demokritov S O, Hillebrands B and Slavin A N 2002 *Phys. Rev.* B **66** 132402

[64] Guslienko K Y, Chantrell R W and Slavin A N 2003 *Phys. Rev.* B **68** 024422

[65] Guslienko K Y and Slavin A N 2005 *Phys. Rev.* B **72** 014463

[66] Tacchi S, Madami M, Gubbiotti G, Carlotti G, Goolaup S, Adeyeye A O, Singh N and Kostylev M P 2010 *Phys. Rev.* B **82** 184408

[67] Brongersma M L, Hartman J W and Atwater H A 2000 *Phys. Rev.* B **62** R16356

[68] Maier S A, Brongersma M L, Kik P G and Atwater H A 2002 *Phys. Rev.* B **65** 193408

[69] Dvornik M and Kruglyak V V 2011 *Phys. Rev.* B **84** 140405

[70] Kostylev M P, Stashkevich A A and Sergeeva N A 2004 *Phys. Rev.* B **69** 064408

[71] Zighem F, Roussigne Y, Cherif S M and Moch P 2007 *J. Phys.: Condens. Matter* **19** 176220

[72] Topp J, Heitmann D and Grundler D 2009 *Phys. Rev.* B **80** 174421

[73] Jorzick J, Demokritov S O, Hillebrands B, Bailleul M, Fermon C, Guslienko K Y, Slavin A N, Berkov D V and Gorn N L 2002 *Phys. Rev. Lett.* **88** 047204

[74] Bayer C, Demokritov S O, Hillebrands B and Slavin A N 2003 *Appl. Phys. Lett.* **82** 607

[75] Kostylev M P, Gubbiotti G, Hu J G, Carlotti G, Ono T and Stamps R L 2007 *Phys. Rev.* B **76** 054422

[76] Kuanr B, Veerakumar V, Malkinski L, Kuanr A, Camley R and Celinski Z 2009 *IEEE Trans. Magn.* **45** 3550

[77] Paz E, Cebollada F, Palomares F J, Gonzalez J M, Martins J S, Santos N M and Sobolev N A 2012 *J. Appl. Phys.* **111** 123917

[78] Adeyeye A O and Jain S 2011 *J. Appl. Phys.* **109** 07B903

[79] Huber R and Grundler D 2011 *Proc. SPIE* **8100** 81000D

[80] Han D S, Vogel A, Jung H, Lee K S, Weigand M, Stoll H, Schütz G, Fischer P, Meier G and Kim S K 2013 *Sci. Rep.* **3** 2262

[81] Sokolovsky M and Krawczyk M 2011 *J. Nanopart. Res.* **13** 6085

[82] Zhang V L, Ma F S, Pan H H, Lin C S, Lim H S, Ng S C, Kuok M H, Jain S and Adeyeye A O 2012 *Appl. Phys. Lett.* **100** 163118

[83] Lin C S, Lim H S, Zhang V L, Wang Z K, Ng S C, Kuok M H, Cottam M G, Jain S and Adeyeye A O 2012 *J. Appl. Phys.* **111** 033920

[84] Zhang V L, Lim H S, Lin C S, Wang Z K, Ng S C, Kuok M H, Jain S, Adeyeye A O and Cottam M G 2011 *Appl. Phys. Lett.* **99** 143118

[85] Sokolovskyy M L, Klos J W, Mamica S and Krawczyk M 2012 *J. Appl. Phys.* **111** 07C515

[86] Ma F, Lim H, Zhang V, Ng S and Kuok M 2012 *Nanoscale Res. Lett.* **7** 498

[87] Kim S K, Lee K S and Han D S 2009 *Appl. Phys. Lett.* **95** 082507

[88] Klos J W, Kumar D, Krawczyk M and Barman A 2013 *Sci. Rep.* **3** 2444

[89] Al-Wahsh H, Akjouj A, Djafari-Rouhani B and Dobrzynski L 2011 *Surf. Sci. Rep.* **66** 29

[90] Tkachenko V S, Kuchko A N, Dvornik M and Kruglyak V V 2012 *Appl. Phys. Lett.* **101** 52402

[91] Kumar D, Sabareesan P, Wang W, Fangohr H and Barman A 2013 *J. Appl. Phys.* **114** 023910

[92] Tkachenko V S, Kruglyak V V and Kuchko A N 2010 *Phys. Rev.* B **81** 024425

[93] Al-Wahsh H 2010 *Eur. Phys. J.* B **73** 527

[94] Djafari-Rouhani B, Al-Wahsh H, Akjouj A and Dobrzynski L 2011 *J. Phys.: Conf. Ser.* **303** 012017

[95] Lee K S, Han D S and Kim S K 2009 *Phys. Rev. Lett.* **102** 127202

[96] Kim S K 2010 *J. Phys. D: Appl. Phys.* **43** 264004

[97] Chumak A V *et al* 2009 *Appl. Phys. Lett.* **95** 262508

[98] Arikan M, Au Y, Vasile G, Ingvarsson S and Kruglyak V V 2013 *J. Phys. D: Appl. Phys.* **46** 135003

[99] Kłos J W, Kumar D, Romero-Vivas J, Fangohr H, Franchin M, Krawczyk M and Barman A 2012 *Phys. Rev.* B **86** 184433

[100] Wang Q, Zhong Z, Jin L, Tang X, Bai F, Zhang H and Beach G S 2013 *J. Magn. Magn. Mater.* **340** 23

[101] Owens J M, Collins J H, Smith C V and Chiang I I 1977 *Appl. Phys. Lett.* **31** 781

[102] Reed K, Owens J and Carter R 1985 *Circuits Syst. Signal Process.* **4** 157

[103] Brinlee W R, Owens J M, Smith C V Jr and Carter R L 1981 *J. Appl. Phys.* **52** 2276

[104] Grigorieva N and Kalinikos B 2009 *Tech. Phys.* **54** 1196

[105] Dokukin M E, Togo K and Inoue M 2008 *J. Magn. Soc. Japan* **32** 103

[106] Inoue M, Baryshev A, Takagi H, Lim P B, Hatafuku K, Noda J and Togo K 2011 *Appl. Phys. Lett.* **98** 132511

[107] Bankov S and Nikitov S 2007 *J. Commun. Technol. Electron.* **52** 1201

[108] Gulyaev Yu V, Nikitov S and Plessky V 1982 *Tech. Phys. J.* **52** 799

[109] Vysotskii S, Beginin E, Nikitov S, Pavlov E and Filimonov Y 2011 *Tech. Phys. Lett.* **37** 1024

[110] Beginin E N, Filimonov Y A, Pavlov E S, Vysotskii S L and Nikitov S A 2012 *Appl. Phys. Lett.* **100** 252412

[111] Vysotskii S, Nikitov S, Pavlov E and Filimonov Y 2013 *J. Commun. Technol. Electron.* **58** 347

[112] Mruczkiewicz M, Krawczyk M, Gubbiotti G, Tacchi S, Filimonov Y A, Kalyabin D V, Lisenkov I V and Nikitov S A 2013 *New J. Phys.* **15** 113023

[113] Saha S, Mandal R, Barman S, Kumar D, Rana B, Fukuma Y, Sugimoto S, Otani Y and Barman A 2013 *Adv. Funct. Mater.* **23** 2378
[114] Rana B and Barman A 2013 *SPIN* **03** 1330001
[115] Zivieri R 2012 *Solid State Phys.* **63** 151
[116] Schwarze T, Huber R, Duerr G and Grundler D 2012 *Phys. Rev.* B **85** 134448
[117] Gubbiotti G, Tacchi S, Madami M, Carlotti G, Jain S, Adeyeye A O and Kostylev M P 2012 *Appl. Phys. Lett.* **100** 162407
[118] Duerr G, Madami M, Neusser S, Tacchi S, Gubbiotti G, Carlotti G and Grundler D 2011 *Appl. Phys. Lett.* **99** 202502
[119] Tacchi S, Duerr G, Klos J W, Madami M, Neusser S, Gubbiotti G, Carlotti G, Krawczyk M and Grundler D 2012 *Phys. Rev. Lett.* **109** 137202
[120] Wolf M, Patschureck C and Sch R 2011 *J. Magn. Magn. Mater.* **323** 1703
[121] Gubbiotti G, Madami M, Tacchi S, Carlotti G and Okuno T 2006 *J. Appl. Phys.* **99** 08C701
[122] Kruglyak V V, Keatley P S, Neudert A, Hicken R J, Childress J R and Katine J A 2010 *Phys. Rev. Lett.* **104** 027201
[123] Dantas C C 2011 *Physica* E **44** 675
[124] Politi P and Pini M G 2002 *Phys. Rev.* B **66** 214414
[125] Galkin A Y, Ivanov B A and Zaspel C E 2006 *Phys. Rev.* B **74** 144419
[126] Tacchi S *et al* 2011 *Phys. Rev. Lett.* **107** 127204
[127] Awad A A, Aranda G R, Dieleman D, Guslienko K Y, Kakazei G N, Ivanov B A and Aliev F G 2010 *Appl. Phys. Lett.* **97** 132501
[128] Barman A, Barman S, Kimura T, Fukuma Y and Otani Y 2010 *J. Phys. D: Appl. Phys.* **43** 422001
[129] Montoncello F and Giovannini L 2012 *Appl. Phys. Lett.* **100** 182406
[130] Shibata J and Otani Y 2004 *Phys. Rev.* B **70** 012404
[131] Verba R, Melkov G, Tiberkevich V and Slavin A 2012 *Phys. Rev.* B **85** 014427
[132] Tacchi S, Madami M, Gubbiotti G, Carlotti G, Tanigawa H, Ono T and Kostylev M P 2010 *Phys. Rev.* B **82** 024401
[133] Kumar N and Prabhakar A 2013 *IEEE Trans. Magn.* **49** 1024
[134] Guslienko K Y and Slavin A N 2000 *J. Appl. Phys.* **87** 6337
[135] Giovannini L, Montoncello F and Nizzoli F 2007 *Phys. Rev.* B **75** 024416
[136] Montoncello F, Tacchi S, Giovannini L, Madami M, Gubbiotti G, Carlotti G, Sirotkin E, Ahmad E, Ogrin F Y and Kruglyak V V 2013 *Appl. Phys. Lett.* **102** 202411
[137] Barman A and Barman S 2009 *Phys. Rev.* B **79** 144415
[138] Mahato B K, Rana B, Mandal R, Kumar D, Barman S, Fukuma Y, Otani Y and Barman A 2013 *Appl. Phys. Lett.* **102** 192402
[139] Rana B, Kumar D, Barman S, Pal S, Mandal R, Fukama Y, Otani Y, Sugimoto S and Barman A 2012 *J. Appl. Phys.* **111** 07D503
[140] Kostylev M, Zhong S, Ding J and Adeyeye A O 2013 *J. Appl. Phys.* **114** 113910
[141] Tse D H Y, Steinmuller S J, Trypiniotis T, Anderson D, Jones G A C, Bland J A C and Barnes C H W 2009 *Phys. Rev.* B **79** 054426
[142] Tacchi S, Madami M, Gubbiotti G, Carlotti G, Adeyeye A O, Neusser S, Botters B and Grundler D 2010 *IEEE Trans. Magn.* **46** 1440
[143] Gulyaev Y, Nikitov S, Zhivotovskii L, Klimov A, Tailhades P, Presmanes L, Bonningue C, Tsai C, Vysotskii S and Filimonov Y 2003 *JETP Lett.* **77** 567
[144] Ding J, Tripathy D and Adeyeye A O 2011 *J. Appl. Phys.* **109** 07D304
[145] Tacchi S, Madami M, Gubbiotti G, Carlotti G, Adeyeye A, Neusser S, Botters B and Grundler D 2010 *IEEE Trans. Magn.* **46** 172
[146] Bhat V, Woods J, Long L D, Hastings J, Metlushko V, Rivkin K, Heinonen O, Sklenar J and Ketterson J 2012 *Physica* C **479** 83
[147] Yu C, Pechan M J and Mankey G J 2003 *Appl. Phys. Lett.* **83** 3948
[148] Martens S, Albrecht O, Nielsch K and Gorlitz D 2009 *J. Appl. Phys.* **105** 07C113
[149] Yu M, Malkinski L, Spinu L, Zhou W and Whittenburg S 2007 *J. Appl. Phys.* **101** 09F501
[150] Martyanov O N, Yudanov V F, Lee R N, Nepijko S A, Elmers H J, Hertel R, Schneider C M and Schönhense G 2007 *Phys. Rev.* B **75** 174429
[151] Barman A 2010 *J. Phys. D: Appl. Phys.* **43** 195002
[152] Semenova E K and Berkov D V 2013 *J. Appl. Phys.* **114** 013905
[153] Zivieri R and Giovannini L 2012 *Metamaterials* **6** e127
[154] Neusser S, Duerr G, Tacchi S, Madami M, Sokolovskyy M L, Gubbiotti G, Krawczyk M and Grundler D 2011 *Phys. Rev.* B **84** 094454
[155] Kostylev M, Gubbiotti G, Carlotti G, Socino G, Tacchi S, Wang C, Singh N, Adeyeye A O and Stamps R L 2008 *J. Appl. Phys.* **103** 07C507
[156] Yu C, Pechan M J, Burgei W A and Mankey G J 2004 *J. Appl. Phys.* **95** 6648
[157] Deshpande N G, Seo M S, Jin X R, Lee S J, Lee Y P, Rhee J Y and Kim K W 2010 *Appl. Phys. Lett.* **96** 122503
[158] Mandal R, Saha S, Kumar D, Barman S, Pal S, Kaustuv D, Raychaudhuri A K, Fukuma Y, Otani Y and Barman A 2012 *ACS Nano* **6** 3397
[159] Neusser S, Duerr G, Bauer H G, Tacchi S, Madami M, Woltersdorf G, Gubbiotti G, Back C H and Grundler D 2010 *Phys. Rev. Lett.* **105** 067208
[160] Zivieri R *et al* 2012 *Phys. Rev.* B **85** 012403
[161] McPhail S, Gürtler C M, Shilton J M, Curson N J and Bland J A C 2005 *Phys. Rev.* B **72** 094414
[162] Pechan M J, Yu C, Compton R L, Park J P and Crowell P A 2005 *J. Appl. Phys.* **97** 10J903
[163] Neusser S, Botters B, Becherer M, Schmitt-Landsiedel D and Grundler D 2008 *Appl. Phys. Lett.* **93** 122501
[164] Hu C L, Magaraggia R, Yuan H Y, Chang C S, Kostylev M, Tripathy D, Adeyeye A O and Stamps R L 2011 *Appl. Phys. Lett.* **98** 262508
[165] Sklenar J, Bhat V S, DeLong L E, Heinonen O and Ketterson J B 2013 *Appl. Phys. Lett.* **102** 152412
[166] Krivoruchko V N and Marchenko A I 2011 *J. Appl. Phys.* **109** 083912
[167] Krivoruchko V and Marchenko A 2012 *J. Magn. Magn. Mater.* **324** 3087
[168] Ding J, Tripathy D and Adeyeye A O 2012 *Europhys. Lett.* **98** 16004
[169] Wang Q, Jin L, Tang X, Bai F, Zhang H and Zhong Z 2012 *IEEE Trans. Magn.* **48** 3246
[170] Lenk B, Abeling N, Panke J and Munzenberg M 2012 *J. Appl. Phys.* **112** 083921

[171] Bali R, Kostylev M, Tripathy D, Adeyeye A O and Samarin S 2012 *Phys. Rev.* B **85** 104414
[172] Schwarze T and Grundler D 2013 *Appl. Phys. Lett.* **102** 222412
[173] Gubbiotti G, Tacchi S, Madami M, Carlotti G, Jain S, Adeyeye A O and Kostylev M P 2012 *Appl. Phys. Lett.* **100** 162407
[174] Liu X M, Ding J and Adeyeye A O 2012 *Appl. Phys. Lett.* **100** 242411
[175] Klos J W, Sokolovskyy M L, Mamica S and Krawczyk M 2012 *J. Appl. Phys.* **111** 123910
[176] Zhang V L, Hou C G, Pan H H, Ma F S, Kuok M H, Lim H S, Ng S C, Cottam M G, Jamali M and Yang H 2012 *Appl. Phys. Lett.* **101** 053102
[177] Hartemann P and Fontaine D 1982 *IEEE Trans. Magn.* **18** 1595
[178] Hartemann P 1988 *J. Appl. Phys.* **63** 2742
[179] Jaworowicz J *et al* 2009 *Appl. Phys. Lett.* **95** 022502
[180] Maziewski A *et al* 2012 *Phys. Rev.* B **85** 054427
[181] Hartemann P 1987 *J. Appl. Phys.* **62** 2111
[182] Ma F S, Lim H S, Wang Z K, Piramanayagam S, Ng S C and Kuok M H 2011 *IEEE Trans. Magn.* **47** 2689
[183] Ma F S, Lim H S, Zhang V L, Wang Z K, Piramanayagam S, Ng S C and Kuok M H 2012 *Nanosci. Nanotechnol. Lett.* **4** 663
[184] Sykes C G, Adam J D and Collins J H 1976 *Appl. Phys. Lett.* **29** 388
[185] Seshadri S R 1978 *J. Appl. Phys.* **49** 6079
[186] Chang N S and Matsuo Y 1979 *Appl. Phys. Lett.* **35** 352
[187] Castera J and Hartemann P 1982 *IEEE Trans. Magn.* **18** 1601
[188] Shanthi S, Alphones A and Lye K M 2000 *Microw. Opt. Technol. Lett.* **24** 52
[189] Vysotski S L, Nikitov S A and Filimonov Y A 2005 *J. Exp. Theor. Phys.* **101** 547
[190] Chumak A V, Serga A A, Hillebrands B and Kostylev M P 2008 *Appl. Phys. Lett.* **93** 022508
[191] Vysotsky S, Nikitov S, Novitskii N, Stognii A and Filimonov Y 2011 *Tech. Phys.* **56** 308–10
[192] Grishin S, Beginin E, Dulin Y, Nikitov S and Sharaevskii Y 2012 *Tech. Phys. Lett.* **38** 638
[193] Chuang V P, Jung W, Ross C A, Cheng J Y, Park O H and Kim H C 2008 *J. Appl. Phys.* **103** 074307
[194] Liu X M, Ding J, Kakazei G N and Adeyeye A O 2013 *Appl. Phys. Lett.* **103** 062401
[195] Navarro E, Huttel Y, Clavero C, Cebollada A and Armelles G 2004 *Phys. Rev.* B **69** 224419
[196] Deshpande N G, Seo M S, Lee S J, Chen L Y, Kim K W, Rhee J Y, Kim Y H and Lee Y P 2012 *J. Appl. Phys.* **111** 013906
[197] Deshpande N G, Hwang J S, Kim K W, Rhee J Y, Kim Y H, Chen L Y and Lee Y P 2012 *Appl. Phys. Lett.* **100** 222403
[198] Tsutsumi M, Sakagouchi Y and Kumagai N 1977 *IEEE Trans. Microw. Theory Tech.* **25** 224
[199] Tsutsumi M, Sakaguchi Y and Kumagai N 1977 *Appl. Phys. Lett.* **31** 779
[200] Tsutsumi M and Kumagai N 1982 *J. Appl. Phys.* **53** 5959
[201] Chumak A V, Serga A A, Wolff S, Hillebrands B and Kostylev M P 2009 *J. Appl. Phys.* **105** 083906
[202] Chi K H, Zhu Y, Mao R W, Dolas J P and Tsai C S 2011 *J. Appl. Phys.* **109** 07D320
[203] Chi K, Yun Z, Rongwei M, Nikitov S, Gulyaev Y and Tsai C 2011 *IEEE Trans. Magn.* **47** 3708
[204] Maeda A and Susaki M 2006 *IEEE Trans. Magn.* **42** 3096
[205] Maeda A and Susaki M 2007 *Phys. Status Solidi* c **4** 4396
[206] Vysotskii S, Nikitov S, Pavlov E and Filimonov Y 2010 *J. Commun. Technol. Electron.* **55** 800
[207] Chumak A V, Serga A A, Wolff S, Hillebrands B and Kostylev M P 2009 *Appl. Phys. Lett.* **94** 172511
[208] Carter R, Smith C and Owens J 1980 *IEEE Trans. Magn.* **16** 1159
[209] Seshadri S R and Tsai M C 1981 *J. Appl. Phys.* **52** 6401
[210] Seshadri S R and Tsai M C 1984 *J. Appl. Phys.* **56** 501
[211] Filimonov Y, Pavlov E, Vystostkii S and Nikitov S 2012 *Appl. Phys. Lett.* **101** 242408
[212] Nikitov S A, Tsai C S, Gulyaev Y V, Filimonov Y A, Volkov A I, Vysotskii S L and Tailhades P 2004 *Mater. Res. Soc. Symp. Proc.* **834** J.2.2
[213] Chi K, Zhu Y, Rongwei M, Nikitov S, Gulyaev Y and Tsai C 2013 *IEEE Trans. Magn.* **49** 1000
[214] Kolodin P and Hillebrands B 1996 *J. Magn. Magn. Mater.* **161** 199
[215] Chang N S and Erkin S 1987 *J. Appl. Phys.* **61** 4124
[216] Nguyen H T and Cottam M G 2012 *J. Appl. Phys.* **111** 07D122
[217] Barsukov I *et al* 2011 *Phys. Rev.* B **84** 140410
[218] Landeros P and Mills D L 2012 *Phys. Rev.* B **85** 054424
[219] Boucher V, Lacroix C, Carignan L P, Yelon A and Menard D 2011 *Appl. Phys. Lett.* **98** 112502
[220] Kou X, Fan X, Dumas R K, Lu Q, Zhang Y, Zhu H, Zhang X, Liu K and Xiao J Q 2011 *Adv. Mater.* **23** 1393
[221] Saib A, Darques M, Piraux L, Vanhoenacker-Janvier D and Huynen I 2005 *J. Phys. D: Appl. Phys.* **38** 2759
[222] Podbielski J, Giesen F, Berginski M, Hoyer N and Grundler D 2005 *Superlatt. Microstruct.* **37** 341
[223] Saib A, Vanhoenacker-Janvier D, Huynen I, Encinas A, Piraux L, Ferain E and Legras R 2003 *Appl. Phys. Lett.* **83** 2378
[224] Giesen F, Podbielski J, Korn T, Steiner M, van Staa A and Grundler D 2005 *Appl. Phys. Lett.* **86** 112510
[225] Giesen F, Podbielski J, Botters B and Grundler D 2007 *Phys. Rev.* B **75** 184428
[226] Bhat V, Woods J, De Long L, Hastings J, Sklenar J, Ketterson J and Pechan M 2013 *IEEE Trans. Magn.* **49** 1029
[227] Ding J, Kostylev M and Adeyeye A O 2011 *Phys. Rev.* B **84** 054425
[228] Ding J and Adeyeye A O 2013 *Adv. Funct. Mater.* **23** 1684
[229] Livesey K L, Ding J, Anderson N R, Camley R E, Adeyeye A O, Kostylev M P and Samarin S 2013 *Phys. Rev.* B **87** 064424
[230] Huber R, Krawczyk M, Schwarze T, Yu H, Duerr G, Albert S and Grundler D 2013 *Appl. Phys. Lett.* **102** 012403
[231] Topp J, Duerr G, Thurner K and Grundler D 2011 *Pure Appl. Chem.* **83** 1989
[232] Ding J, Kostylev M and Adeyeye A O 2012 *Appl. Phys. Lett.* **100** 073114
[233] Gubbiotti G, Tacchi S, Madami M, Carlotti G, Adeyeye A, Samarin S and Kostylev M 2013 *IEEE Trans. Magn.* **49** 3089
[234] Zivieri R, Vavassori P, Giovannini L, Nizzoli F, Fullerton E E, Grimsditch M and Metlushko V 2002 *Phys. Rev.* B **65** 165406
[235] Verba R, Melkov G, Tiberkevich V and and Slavin A 2012 *Appl. Phys. Lett.* **100** 192412

[236] Verba R, Tiberkevich V, Guslienko K, Melkov G and Slavin A 2013 *Phys. Rev.* B **87** 134419
[237] Adeyeye A, Jain S and Ren Y 2011 *IEEE Trans. Magn.* **47** 1639
[238] Saha S, Barman S, Ding J, Adeyeye A O and Barman A 2013 *Appl. Phys. Lett.* **102** 242409
[239] Ding J and Adeyeye A O 2012 *Appl. Phys. Lett.* **101** 103117
[240] Jain S, Kostylev M and Adeyeye A O 2010 *Phys. Rev.* B **82** 214422
[241] Shimon G, Adeyeye A O and Ross C A 2012 *Appl. Phys. Lett.* **101** 083112
[242] Emtage P R and Daniel M R 1984 *Phys. Rev.* B **29** 212
[243] Camley R E, Rahman T S and Mills D L 1983 *Phys. Rev.* B **27** 261
[244] Grünberg P and Mika K 1983 *Phys. Rev.* B **27** 2955
[245] Camley R E and Stamps R L 1993 *J. Phys.: Condens. Matter* **5** 3727
[246] Hillebrands B 1990 *Phys. Rev.* B **41** 530
[247] Kruglyak V and Hicken R 2006 *J. Magn. Magn. Mater.* **2006** 191
[248] Sy H K and Chen F 1994 *Phys. Rev.* B **50** 3411
[249] Zhu R H, Peng H Y, Zhang M H and Chen Y Q 2009 *Physica* B **404** 2086
[250] Deng D S, Jin X F and Tao R 2002 *Phys. Rev.* B **66** 104435
[251] Camley R E and Cottam M G 1987 *Phys. Rev.* B **35** 189
[252] Gao H and Wang X Z 1997 *Phys. Rev.* B **55** 12424
[253] Oliveros M C, Almeida N S, Tilley D R, Thomas J and Camley R E 1992 *J. Phys.: Condens. Matter* **4** 8497
[254] Wang X Z and Tilley D R 1994 *Phys. Rev.* B **50** 13472
[255] Krawczyk M 2008 *IEEE Trans. Magn.* **44** 2854
[256] Barnas J 1988 *J. Phys. C: Solid State Phys.* **21** 1021
[257] Cottam M G and Tilley D R 1989 *Introduction to Surface and Superlattice Excitations* (Cambridge: Cambridge University Press)
[258] Schwenk D, Fishman F and Schwabl F 1988 *Phys. Rev.* B **38** 11618
[259] Kruglyak V and Kuchko A 2003 *Physica* B **339** 130
[260] Barnas J 1988 *J. Phys. C: Solid State Phys.* **21** 4097
[261] Amiri P K and Rejaei B 2006 *J. Appl. Phys.* **100** 03909
[262] Barnaś J 1992 *Phys. Rev.* B **45** 10427
[263] Swirkowicz R 1996 *Phys. Status Solidi* b **195** 267
[264] Anselmo D H A L and Albuquerque E L 1996 *Phys. Status Solidi* b **98** 827
[265] Kruglyak V, Kuchko A and Finokhin V 2004 *Phys. Solid State* **46** 867
[266] Klos J W and Tkachenko V S 2013 *J. Appl. Phys.* **113** 133907
[267] Kueny A, Khan M R, Schuller I K and Grimsditch M 1984 *Phys. Rev.* B **29** 2879
[268] Iskhakov R S, Stolyar S V, Chekanova L A and Chizhik M V 2012 *Phys. Solid State* **54** 748
[269] Hillebrands B, Harzer J V, Güntherodt G, England C D and Falco C M 1990 *Phys. Rev.* B **42** 6839
[270] van Stapele R P, Greidanus F J A M and Smits J W 1985 *J. Appl. Phys.* **57** 1282
[271] Iskhakov R S, Stolyar S V, Chizhik M V and Chekanova L A 2011 *JETP Lett.* **94** 301
[272] Ignatchenko V A, Mankov Y I and Maradudin A A 2000 *Phys. Rev.* B **62** 2181
[273] Ignatchenko V A, Mankov Y I and Maradudin A A 2001 *Phys. Rev.* B **65** 024207
[274] Kruglyak V and Kuchko A 2002 *Phys. Met. Metallogr.* **93** 511
[275] Krawczyk M, Puszkarski H, Levy J C S and Mercier D 2003 *J. Phys.: Condens. Matter* **15** 2449
[276] Ignatchenko V and Laletin O 2004 *Phys. Solid State* **46** 2292–300
[277] Tkachenko V S, Kruglyak V V and Kuchko A N 2006 *J. Magn. Magn. Mater.* **307** 48
[278] Tkachenko V S, Kruglyak V V and Kuchko A N 2009 *Metamaterials* **3** 28
[279] Hillebrands B 1988 *Phys. Rev.* B **37** 9885
[280] Kruglyak V and Kuchko A 2004 *J. Magn. Magn. Mater.* **272** 302
[281] Vasseur J O, Dobrzynski L, Djafari-Rouhani B and Puszkarski H 1996 *Phys. Rev.* B **54** 1043
[282] Krawczyk M and Puszkarski H 1998 *Acta Phys. Pol.* A **93** 805
[283] Puszkarski H and Krawczyk M 2003 *Solid State Phenom.* **94** 125
[284] Cao Y, Yun G, Liang X and Bai N 2010 *J. Phys. D: Appl. Phys.* **43** 305005
[285] Mamica S, Krawczyk M and Klos J W 2012 *Adv. Condens. Matter Phys.* **2012** 1
[286] Yang H, Yun G and Cao Y 2011 *J. Phys. D: Appl. Phys.* **44** 455001
[287] Tiwari R P and Stroud D 2010 *Phys. Rev.* B **81** 220403
[288] Yang H, Yun G and Cao Y 2012 *J. Appl. Phys.* **111** 013908
[289] Yang H, Yun G and Cao Y 2012 *J. Appl. Phys.* **112** 103911
[290] Arias R and Mills D L 2004 *Phys. Rev.* B **70** 104425
[291] Arias R, Chu P and Mills D L 2005 *Phys. Rev.* B **71** 224410
[292] Chu P, Mills D L and Arias R 2006 *Phys. Rev.* B **73** 094405
[293] Tartakovskaya E, Kreuzpaintner W and Schreyer A 2008 *J. Appl. Phys.* **103** 023913
[294] Mitsumata C, Tomita S, Hagiwara M and Akamatsu K 2010 *J. Phys.: Condens. Matter* **22** 016005
[295] Mitsumata C and Tomita S 2011 *Phys. Rev.* B **84** 174421
[296] Plumer M L, van Lierop J, Southern B W and Whitehead J P 2010 *J. Phys.: Condens. Matter* **22** 296007
[297] Krawczyk M and Puszkarski H 2006 *Cryst. Res. Technol.* **41** 547
[298] Krawczyk M and Puszkarski H 2006 *J. Appl. Phys.* **100** 073905
[299] Krawczyk M, Klos J, Sokolovskyy M L and Mamica S 2010 *J. Appl. Phys.* **108** 093909
[300] Romero Vivas J, Mamica S, Krawczyk M and Kruglyak V V 2012 *Phys. Rev.* B **86** 144417
[301] Biotteau G, Hennion M, Moussa F, Rodriguez-Carvajal J, Pinsard L, Revcolevschi A, Mukovskii Y M and Shulyatev D 2001 *Phys. Rev.* B **64** 104421
[302] Kasyutich O, Sarua A and Schwarzacher W 2008 *J. Phys. D: Appl. Phys.* **41** 134022
[303] Okuda M, Eloi J C, Jones S E W, Sarua A, Richardson R M and Schwarzacher W 2012 *Nanotechnology* **23** 415601
[304] Kruglyak V *et al* 2012 Magnonic metamaterials *Metamaterial* (Rijeka, Croatia: Intech) pp 1–31
[305] Mamica S 2013 *J. Appl. Phys.* **114** 043912
[306] Mamica S, Krawczyk M, Sokolovskyy M L and Romero-Vivas J 2012 *Phys. Rev.* B **86** 144402
[307] Kostylev M *et al* 2012 *Phys. Rev.* B **86** 184431
[308] Grigoriev S V *et al* 2009 *Phys. Rev.* B **79** 045123
[309] Daub M, Knez M, Goesele U and Nielsch K 2007 *J. Appl. Phys.* **101** 09J111
[310] Huber R, Schwarze T, Berberich P, Rapp T and Grundler D 2011 *Metamaterials 2011: The 5th Int. Congr. on*

Advanced Electromagnetic Materials in Microwaves and Optics p 588 ISSN 978-952-67611-0-7 Metamorphose-VI
[311] Pascu O, Caicedo J M, Lopez-Garcia M, Canalejas V, Blanco A, Lopez C, Arbiol J, Fontcuberta J, Roig A and Herranz G 2011 *Nanoscale* **3** 4811
[312] Perzlmaier K, Woltersdorf G and Back C H 2008 *Phys. Rev.* B **77** 054425
[313] Schultheiss H, Sandweg C W, Obry B, Hermsdörfer S, Schäfer S, Leven B and Hillebrands B 2008 *J. Phys. D: Appl. Phys.* **41** 164017
[314] Nembach H T, Shaw J M, Boone C T and Silva T J 2013 *Phys. Rev. Lett.* **110** 117201
[315] Dvornik M, Vansteenkiste A and Van Waeyenberge B 2013 *Phys. Rev.* B **88** 054427
[316] Ding J, Kostylev M and Adeyeye A O 2011 *Phys. Rev. Lett.* **107** 047205
[317] Huber R, Schwarze T and Grundler D 2013 *Phys. Rev.* B **88** 100405(R)
[318] Maier S A and Atwater H A 2005 *J. Appl. Phys.* **98** 011101
[319] Khurgin J B and Boltasseva A 2012 *Mater. Res. Soc. Bull.* **37** 768
[320] Arias R and Mills D L 1999 *Phys. Rev.* B **60** 7395
[321] Gilmore K, Idzerda Y U and Stiles M D 2007 *Phys. Rev. Lett.* **99** 027204
[322] Fähnle M and Illg C 2011 *J. Phys.: Condens. Matter* **23** 493201
[323] Sun Y, Song Y Y, Chang H, Kabatek M, Jantz M, Schneider W, Wu M, Schultheiss H and Hoffmann A 2012 *Appl. Phys. Lett.* **101** 152405
[324] d'Allivy Kelly O *et al* 2013 *Appl. Phys. Lett.* **103** 082408
[325] Kajiwara Y *et al* 2010 *Nature* **464** 262
[326] Wang Z, Sun Y, Wu M, Tiberkevich V and Slavin A 2011 *Phys. Rev. Lett.* **107** 146602
[327] Demidov V E, Urazhdin S, Ulrichs H, Tiberkevich V, Slavin A, Baither D, Schmitz G and Demokritov S O 2012 *Nature Mater.* **11** 1028
[328] Keatley P S, Gangmei P, Dvornik M, Hicken R J, Grollier J and Ulysse C 2013 *Phys. Rev. Lett.* **110** 187202
[329] Putter S, Mikuszeit N, Vedmedenko E Y and Oepen H P 2009 *J. Appl. Phys.* **106** 043916
[330] Semenova E K *et al* 2013 *Phys. Rev.* B **87** 174432
[331] Dmytriiev O, Kruglyak V V, Franchin M, Fangohr H, Giovannini L and Montoncello F 2013 *Phys. Rev.* B **87** 174422
[332] Di K, Lim H S, Zhang V L, Kuok M H, Ng S C, Cottam M G and Nguyen H T 2013 *Phys. Rev. Lett.* **111** 149701
[333] Lee K S, Han D S and Kim S K 2013 *Phys. Rev. Lett.* **11** 149702
[334] Bishop J E L, Galkin A Y and Ivanov B A 2002 *Phys. Rev.* B **65** 174403
[335] Bhat V S, Sklenar J, Farmer B, Woods J, Hastings J T, Lee S J, Ketterson J B and De Long L E 2013 *Phys. Rev. Lett.* **111** 077201
[336] Costa C, Barbosa P, Filho F B, Vasconcelos M and Albuquerque E 2010 *Solid State Commun.* **150** 2325
[337] Costa C, Vasconcelos M, Barbosa P and Filho F B 2012 *J. Magn. Magn. Mater.* **324** 2315
[338] Grishin S V, Beginin E N, Sharaevskii Y P and Nikitov S A 2013 *Appl. Phys. Lett.* **103** 022408
[339] Forestiere C, Miano G, Rubinacci G and Dal Negro L 2009 *Phys. Rev.* B **79** 085404
[340] Au Y, Dvornik M, Dmytriiev O and Kruglyak V V 2012 *Appl. Phys. Lett.* **100** 172408
[341] Luo C, Johnson S G, Joannopoulos J D and Pendry J B 2002 *Phys. Rev.* B **65** 201104
[342] Zhang X and Liu Z 2004 *Appl. Phys. Lett.* **85** 341
[343] Mizukami S, Zhang X, Kubota T, Naganuma H, Oogane M, Ando Y and Miyazaki T 2011 *Appl. Phys. Express* **4** 013005
[344] Haertinger M, Back C H, Yang S H, Parkin S S P and Woltersdorf G 2013 *J. Phys. D: Appl. Phys.* **46** 175001
[345] Roy K, Bandyopadhyay S and Atulasimha J 2011 *Appl. Phys. Lett.* **99** 063108
[346] Hu J, Yang T N, Chen L Q and Nan C W 2013 *J. Appl. Phys.* **113** 194301
[347] Neusser S, Bauer H G, Duerr G, Huber R, Mamica S, Woltersdorf G, Krawczyk M, Back C H and Grundler D 2011 *Phys. Rev.* B **84** 184411
[348] Ustinov A B, Drozdovskii A V and Kalinikos B A 2010 *Appl. Phys. Lett.* **96** 142513
[349] He P, Gu G and Pan A 2012 *Eur. Phys. J.* B **85 B** 119
[350] Chen N N, Slavin A and Cottom M 1992 *IEEE Trans. Magn.* **28** 3306
[351] Kalinikos B A, Kovshikov N G and Slavin A N 1991 *J. Appl. Phys.* **69** 5712
[352] Wang Q, Shi J and Bao J 1995 *J. Appl. Phys.* **77** 5831
[353] Dragoman M and Jager D 1993 *Appl. Phys. Lett.* **62** 110
[354] Chen N N, Slavin A N and Cottam M G 1993 *Phys. Rev.* B **47** 8667
[355] Kivshar Y S and Agrawal G 2003 *Optical Solitons. From Fibers to Photonic Crystals* (San Diego, CA: Elsevier–Academic)
[356] Mollenauer L F and Gordon J P 2006 *Solitons in Optical Fibers. Fundamentals and Applications* (San Diego, CA: Elsevier–Academic)
[357] Ustinov A, Grigorieva N and Kalinikos B 2008 *JETP Lett.* **88** 31
[358] Ustinov A B, Kalinikos B A, Demidov V E and Demokritov S O 2010 *Phys. Rev.* B **81** 180406
[359] Drozdovskii A, Cherkasskii M, Ustinov A, Kovshikov N and Kalinikos B 2010 *JETP Lett.* **91** 16
[360] Drozdovskii A and Kalinikos B 2012 *JETP Lett.* **95** 357
[361] Beginin E, Grishin S, Nikitov S, Sharaevskii Y and Sheshukova S 2011 *Tech. Phys. Lett.* **37** 1065
[362] Kittel C 1958 *Phys. Rev.* **110** 836
[363] Eshbach J R 1962 *Phys. Rev. Lett.* **8** 357
[364] Armelles G, Cebollada A, García-Martín A and González M U 2013 *Adv. Opt. Mater.* **1** 10
[365] Temnov V V 2012 *Nature Photon.* **6** 728
[366] Camley R E and Scott R Q 1978 *Phys. Rev.* B **17** 4327
[367] Gulyaev Y and Zil'berman P 1988 *Sov. Phys. J.* **31** 860
[368] Comstock R L and Wigen P E 1965 *J. Appl. Phys.* **36** 2426
[369] Filimonov Y and Khivintsev Y 2002 *Tech. Phys.* **47** 38
[370] Kim J W, Vomir M and Bigot J Y 2012 *Phys. Rev. Lett.* **109** 166601
[371] Kovalenko O, Pezeril T and Temnov V V 2013 *Phys. Rev. Lett.* **110** 266602
[372] Davis S, Baruth A and Adenwalla S 2010 *Appl. Phys. Lett.* **97** 232507

[373] Schlomann E and Joseph R I 1964 *J. Appl. Phys.* **35** 2382
[374] Weiler M, Dreher L, Heeg C, Huebl H, Gross R, Brandt M S and Goennenwein S T B 2011 *Phys. Rev. Lett.* **106** 117601
[375] Weiler M, Huebl H, Goerg F S, Czeschka F D, Gross R and Goennenwein S T B 2012 *Phys. Rev. Lett.* **108** 176601
[376] Dreher L, Weiler M, Pernpeintner M, Huebl H, Gross R, Brandt M S and Goennenwein S T B 2012 *Phys. Rev.* B **86** 134415
[377] Camley R E 1979 *J. Appl. Phys.* **50** 5272
[378] Bespyatykh Y I, Dikshtein I E, Mal'tzev V P and Nikitov S A 2003 *Phys. Rev.* B **68** 144421
[379] Ignatchenko V A and Laletin O N 2007 *Phys. Rev.* B **76** 104419
[380] Pan H, Zhang V L, Di K, Kuok M H, Lim H S, Ng S C, Singh N and Adeyeye A O 2013 *Nanoscale Res. Lett.* **8** 115
[381] Matar O B, Robillard J F, Vasseur J O, Hladky-Hennion A C, Deymier P A, Pernod P and Preobrazhensky V 2012 *J. Appl. Phys.* **111** 054901
[382] Mednikov A M, Popkov A F, Anisimkin V I, Nam B P, Petrov A A, Spivakov D D and Khe A S 1981 *Pis. Zh. Eksp. Teor. Fiz.* **33** 646
[383] Kryshtal R G and Medved A V 2012 *Appl. Phys. Lett.* **100** 192410
[384] Lyubchanskii I L, Dadoenkova N N, Lyubchanskii M I, Shapovalov E A and Rasing T 2003 *J. Phys. D: Appl. Phys.* **36** R277
[385] Inoue M, Fujikawa R, Baryshev A, Khanikaev A, Lim P B, Uchida H, Aktsipetrov O, Fedyanin A, Murzina T and Granovsky A 2006 *J. Phys. D: Appl. Phys.* **39** R151
[386] Inoue M, Levy M and Baryshev A V (ed) 2013 *Magneto-Optics of Plasmonic Crystals (Springer Series in Materials Science* vol 178) (Berlin: Springer)
[387] Auld B A and Wilson D A 1967 *J. Appl. Phys.* **38** 3331
[388] Tien P, Martin R, Blank S, Wemple S and Varnerin L 1972 *Appl. Phys. Lett.* **21** 207
[389] Tsai C S, Young D, Chen W, Adkins L, Lee C C and Glass H 1985 *Appl. Phys. Lett.* **47** 651
[390] Pu Y, Wang C L and Tsai C 1991 *IEEE Photon. Technol. Lett.* **3** 462
[391] Stashkevich A 1989 *Sov. Phys. J.* **32** 241
[392] Tsai C S, Lin Y S, Su J and Calciu S R 1997 *Appl. Phys. Lett.* **71** 3715
[393] Temnov V V, Armelles G, Woggon U, Guzatov D, Cebollada A, Garcia-Martin A, Garcia-Martin J M, Thomay T, Leitenstorfer A and Bratschitsch R 2010 *Nature Photon.* **4** 107
[394] Ferreiro-Vila E, García-Martín J M, Cebollada A, Armelles G and González M U 2013 *Opt. Express* **21** 4917
[395] Torrado J F, Papaioannou E T, Ctistis G, Patoka P, Giersig M, Armelles G and Garcia-Martin A 2010 *Phys. Status Solidi (RRL)-Rapid Res. Lett* **4** 271
[396] Kostylev N, Maksymov I S, Adeyeye A O, Samarin S, Kostylev M and Williams J F 2013 *Appl. Phys. Lett.* **102** 121907
[397] Jarufe C and Arias R E 2012 *Phys. Rev.* B **85** 205411
[398] Chui S T, Lin Z F, Chang C R and Xiao J 2013 *J. Appl. Phys.* **113** 233910
[399] Fan S 2010 *Nature Photon.* **4** 76
[400] Mikhaylovskiy R V, Hendry E and Kruglyak V V 2010 *Phys. Rev.* B **82** 195446
[401] Mruczkiewicz M, Krawczyk M, Mikhaylovskiy R V and Kruglyak V V 2012 *Phys. Rev.* B **86** 024425
[402] Dmytriiev O *et al* 2012 *Phys. Rev.* B **86** 104405
[403] Spector H 1968 *Solid State Commun.* **6** 811
[404] Schlomann E 1969 *J. Appl. Phys.* **40** 1422
[405] Kornyushin Y V 1970 *Phys. Status Solidi* b **41** 265
[406] Coutinho Filho M D, Miranda L C M and Rezende S M 1973 *Phys. Status Solidi* b **57** 85
[407] Bini M, Filetti P L, Millanta L and Rubino N 1976 *J. Appl. Phys.* **47** 3209
[408] Yukawa T, Ikenoue J, Shingai S and Abe K 1980 *J. Appl. Phys.* **51** 151
[409] Yamada S, Chang N S and Matsuo Y 1982 *J. Appl. Phys.* **53** 5979
[410] Vlaminck V and Bailleul M 2008 *Science* **322** 410
[411] Seo S M, Lee K J, Yang H and Ono T 2009 *Phys. Rev. Lett.* **102** 147202
[412] Xing X J, Yu Y P and Li S W 2009 *Appl. Phys. Lett.* **95** 142508
[413] Zhang S S L and Zhang S 2012 *Phys. Rev. Lett.* **109** 096603
[414] Zhu M, Dennis C L and McMichael R D 2010 *Phys. Rev.* B **81** 140407
[415] Polushkin N I 2011 *Appl. Phys. Lett.* **99** 182502
[416] Mühlbauer S, Binz B, Jonietz F, Pfleiderer C, Rosch A, Neubauer A, Georgii R and Böni P 2009 *Science* **323** 915
[417] Münzer W *et al* 2010 *Phys. Rev.* B **81** 041203
[418] Seki S, Yu X Z, Ishiwata S and Tokura Y 2012 *Science* **336** 198
[419] Rosch A 2012 *Proc. Natl Acad. Sci. USA* **109** 8793
[420] Yu X Z, Kanazawa N, Onose Y, Kimoto K, Zhang W Z, Ishiwata S, Matsui Y and Tokura Y 2011 *Nature Mater.* **10** 106
[421] Jonietz F *et al* 2010 *Science* **330** 1648
[422] Everschor K, Garst M, Binz B, Jonietz F, Mühlbauer S, Pfleiderer C and Rosch A 2012 *Phys. Rev.* B **86** 054432
[423] White J S *et al* 2012 *J. Phys.: Condens. Matter* **24** 432201
[424] Janoschek M, Bernlochner F, Dunsiger S, Pfleiderer C, Böni P, Roessli B, Link P and Rosch A 2010 *Phys. Rev.* B **81** 214436
[425] Petrova O and Tchernyshyov O 2011 *Phys. Rev.* B **84** 214433
[426] Zang J, Mostovoy M, Han J H and Nagaosa N 2011 *Phys. Rev. Lett.* **107** 136804
[427] Mochizuki M 2012 *Phys. Rev. Lett.* **108** 017601
[428] Koralek J D, Meier D, Hinton J P, Bauer A, Parameswaran S A, Vishwanath A, Ramesh R, Schoenlein R W, Pfleiderer C and Orenstein J 2012 *Phys. Rev. Lett.* **109** 247204
[429] Onose Y, Okamura Y, Seki S, Ishiwata S and Tokura Y 2012 *Phys. Rev. Lett.* **109** 037603
[430] Schwarze T, Waizner J, Garst M, Bauer A, Stasinopoulos I, Berger H, Pfeiderer C P and Grundler D 2013 unpublished
[431] Sun L, Cao R X, Miao B F, Feng Z, You B, Wu D, Zhang W, Hu A and Ding H F 2013 *Phys. Rev. Lett.* **110** 167201
[432] Bobeck A H and Della Torre E 1975 *Magnetic Bubbles (Selected Topics in Solid State Physics)* (New York: North-Holland, American Elsevier)

[433] Bobeck A, Bonyhard P and Geusic J 1975 *Proc. IEEE* **63** 1176

[434] Tomlinson J and Wieder H 1975 *Radio Electron. Eng.* **45** 725

[435] Tomas I, Szymczak R A and Kaczer J 1973 *Phys. Status Solidi* a **16** 439

[436] Artman J O and Charap S H 1978 *J. Appl. Phys.* **49** 1587

[437] Klem Z and Kaczér J 1985 *Phys. Status Solidi* a **92** 525

[438] O'Dell T H 1973 *Phil. Mag.* **27** 595

[439] Jirsa M, Kamberský V, Kolodrubec A and Nevøiva M 1987 *Phys. Status Solidi* a **103** 219

[440] Charap S H and Artman J O 1978 *J. Appl. Phys.* **49** 1585

[441] Jirsa M 1990 *Czech. J. Phys.* **40** 209

[442] O'Dell T H 1986 *Rep. Prog. Phys.* **49** 589

[443] Duerr G, Huber R and Grundler D 2012 *J. Phys.: Condens. Matter* **24** 024218

[444] Papworth K 1974 *IEEE Trans. Magn.* **10** 638

[445] Bosse A, Lührmann B, Dötsch H, Sure S and Tolksdorf W 1994 *Phys. Status Solidi* a **141** 417

[446] Fehndrich M and Dötsch H 1996 *Phys. Status Solidi* a **157** 127

[447] Shul'ga N, Doroshenko R and Mal'ginova S 2009 *Phys. Met. Metallogr.* **108** 1

[448] Kostenko V I and Sigal M A 1992 *Phys. Status Solidi* b **170** 569

[449] Ebels U, Buda L, Ounadjela K and Wigen P E 2001 *Phys. Rev.* B **63** 174437

[450] Ebels U, Buda L D, Ounadjela K and Wigen P E 2002 Small amplitude dynamics of nonhomogeneous magnetization distributions: the excitation spectrum of stripe domains *Spin Dynamics in Confined Magnetic Structures I (Springer Topics in Applied Physics)* vol 83, ed B Hillebrands and K Ounadjela (Berlin: Springer) p 167

[451] Wang R F *et al* 2006 *Nature* **439** 303

[452] Heyderman L J and Stamps R L 2013 *J. Phys.: Condens. Matter* **25** 363201

[453] Nisoli C, Moessner R and Schiffer P 2013 *Rev. Mod. Phys.* **85** 1473

[454] Branford W R, Ladak S, Read D E, Zeissler K and Cohen L F 2012 *Science* **335** 1597

[455] Budrikis Z, Politi P and Stamps R L 2012 *New J. Phys.* **14** 045008

[456] Kapaklis V, Arnalds U B, Harman-Clarke A, Papaioannou E T, Karimipour M, Korelis P, Taroni A, Holdsworth P C W, Bramwell S T and Hjörvarsson B 2012 *New J. Phys.* **14** 035009

[457] Sklenar J, Bhat V S, DeLong L E and Ketterson J B 2013 *J. Appl. Phys.* **113** 17B530

[458] Mironov V L, Skorohodov E V and Ermolaeva O L 2012 Ferromagnetic resonance in arrays of anisotropic magnetic nanoparticles on hexagonal lattice *CriMiCo 2012: 22nd Int. Crimean Conf. on Microwave and Telecommunication Technology (IEEE Catalog Number: CFP12788)* p 741

[459] Gliga S, Kakay A, Hertel R and Heinonen O 2013 *Phys. Rev. Lett.* **110** 117205

[460] Mellado P, Petrova O, Shen Y and Tchernyshyov O 2010 *Phys. Rev. Lett.* **105** 187206

[461] Budrikis Z, Morgan J P, Akerman J, Stein A, Politi P, Langridge S, Marrows C H and Stamps R L 2012 *Phys. Rev. Lett.* **109** 037203

[462] Shen Y, Petrova O, Mellado P, Daunheimer S, Cumings J and Tchernyshyov O 2012 *New J. Phys.* **14** 035022

[463] Rovillain P, de Sousa R, Gallais Y, Sacuto A, Méasson M A, Colson D, Forget A, Bibes M, Barthélémy A and Cazayous M 2010 *Nature Mater.* **9** 975

[464] Nan C W, Bichurin M I, Dong S X, Viehland D and Srinivasan G 2008 *J. Appl. Phys.* **103** 031101

[465] Martin L, Crane S P, Chu Y H, Holcomb M B, Gajek M, Huijben M, Yang C H, Balke N and Ramesh R 2008 *J. Phys.: Condens. Matter* **20** 434220

[466] Gunawan V and Stamps R L 2012 *Phys. Rev.* B **85** 104411

[467] Livesey K L 2011 *Phys. Rev.* B **83** 224420

[468] Zhang L, Ren J, Wang J S and Li B 2013 *Phys. Rev.* B **87** 144101

[469] Katsura H, Nagaosa N and Lee P A 2010 *Phys. Rev. Lett.* **104** 066403

[470] Matsumoto R and Murakami S 2011 *Phys. Rev. Lett.* **106** 197202

[471] Shindou R, Matsumoto R, Murakami S and Ohe J I 2013 *Phys. Rev.* B **87** 174427

[472] Shindou R, Ohe J, Matsumoto R, Murakami S and Saitoh E 2013 *Phys. Rev.* B **87** 174402

[473] Chumak A V, Serga A A and Hillebrands B 2013 unpublished

[474] Sklenar J, Bhat V S, Tsai C C, DeLong L E and Ketterson J B 2012 *Appl. Phys. Lett.* **101** 052404

[475] Yu H, Duerr G, Huber R, Bahr M, Schwarze T, Brandl F and Grundler D 2013 *Nature Commun.* **4** 2702

[476] Au Y, Ahmad E, Dmytriiev O, Dvornik M, Davison T and Kruglyak V V 2012 *Appl. Phys. Lett.* **100** 182404

[477] McMichael R D, Twisselmann D J, Bonevich J E, Chen A P, Egelhoff W F Jr and Russek S E 2002 *J. Appl. Phys.* **91** 8647

[478] Ozbay E 2006 *Science* **311** 189